LOS ALAMOS SCIENTIFIC LABORATORY

OF THE UNIVERSITY OF CALIFORNIA

LOS ALAMOS, NEW MEXICO

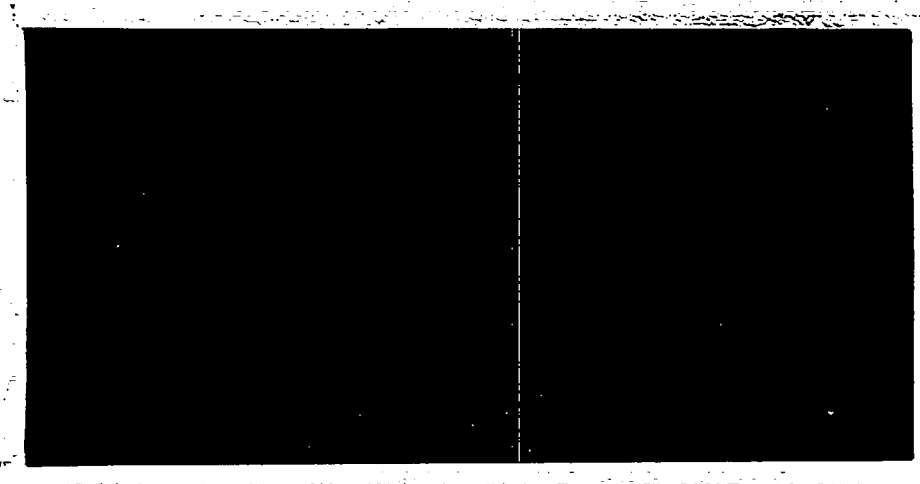

CONTRACT W-7405-ENG.36 WITH THE
U.S. ATOMIC ENERGY COMMISSION

FERENCI

OM T' M

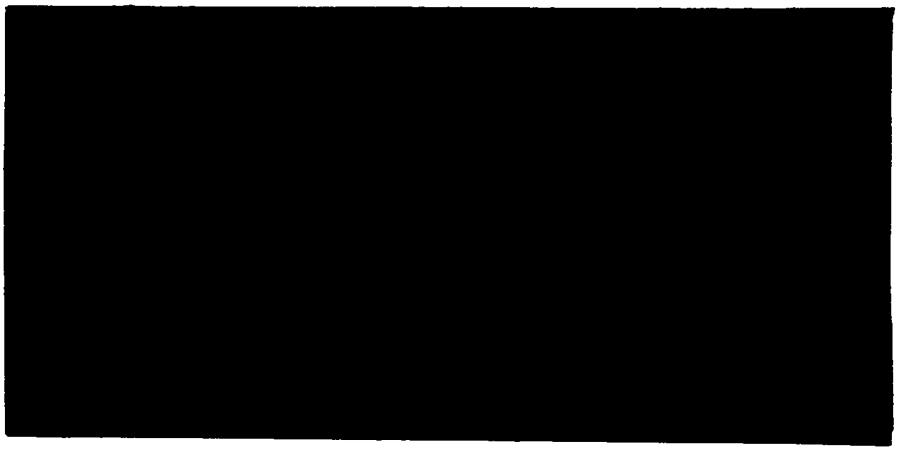

Copy # 20

LOS ALAMOS SCIENTIFIC LABORATORY
of the
UNIVERSITY OF CALIFORNIA

Report written:
December 1954

Report distributed: August 3, 1955

LA-1862

TAYLOR INSTABILITY AND LAMINAR MIXING

by
Garrett Birkhoff

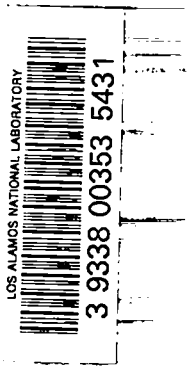

PHYSICS

ABSTRACT

Taylor instability involves five successive stages of mixing: infinitesimal amplitude, finite amplitude, Taylor's "asymptotic" interpenetration by spikes and round-ended columns, breakup of these spikes, ant turbulent mixing. The existing theory of Taylor instability is critically reviewed and extended. This theory covers the first three stages in the growth of periodic disturbances of the interface separating two non-viscous, incompressible fluids. (Using Fourier analysis, the first stage can be treated without assuming periodicity.)

The analysis is based on classical hydrodynamics, supplemented by modern numerical methods. It is indicated how the fourth stage can be treated similarly. However, the fifth stage must be treated by statistical methods, which also throw light on the first four stages. The application of statistical methods to Taylor instability will be treated in a later report.

A supplement to the present report, consisting of appendices which give expanded mathematical discussions of special topics, will also appear later.

I. Introduction

1. The Stability Problem.

"Taylor instability" refers to the principle that "when two superposed fluids of different densities are accelerated in a direction perpendicular to their interface, this surface is stable or unstable according to whether the acceleration is directed from the heavier to the lighter fluid or vice-versa" (Ref. 15, p. 192). Though there are exceptions to this principle (see Sec. 14), it ranks as one of the basic principles of interfacial stability, like the principle of Helmholtz, that discontinuities in the tangential velocity component across an interface tend to make that interface unstable.

In general, it is not possible to separate the two principles for fluid motions because they interact. However, Taylor instability is more important in the case of radically different densities, whereas Helmholtz instability is more important for interfaces separating fluids of nearly equal density (see Sec. 8).

A complete mathematical theory can be given only for infinitesimal (small amplitude) perturbations of certain especially simple types of motion of two fluids separated by an interface. These are:

A. Uniform rectilinear acceleration perpendicular to a plane interface.

B. Impulsive acceleration perpendicular to a plane interface.

C. Periodic acceleration perpendicular to a plane interface.

Clearly, Cases A-C can all be regarded as special cases of variable acceleration perpendicular to a plane interface. There are corresponding cases for:

D. Radial acceleration of a spherical cavity, which may be assumed empty or filled with a compressible gas, and

E. Radial acceleration of a cylindrical cavity.

In Cases A-C of a plane interface, one may combine the normal acceleration with

F. A jump in tangential velocity across the interface.

This gives a still more general problem.

In each of the Cases A-F, the stability problem asks whether a small perturbation of the simplified motion will be amplified or damped. This problem is considered in Part II. This stability problem should not be confused with the mixing problem which asks (in the unstable cases) how far the interpenetration will have progressed in given time.

2. Relevant Physical Variables.

Real fluids are subject not only to inertial forces, arising from their resistance to acceleration, but also to other physical forces such as gravity, surface tension, viscosity, and compressibility.

Such non-inertial forces can often be included in simple motions of types A-F, without increasing their complexity substantially.

This is obviously the case with gravity perpendicular to a plane interface, whether or not a discontinuity in the tangential velocity is involved (see Sec. 4).

It is also the case with surface tension in all cases. It is the case with viscosity, unless a discontinuity in the tangential velocity is involved.

Compressibility can be included in the case of constant acceleration perpendicular to a plane interface, which can be reduced to the hydrostatic case, as in Sec. 4. But in all other cases it gives rise to compression waves, which are hard to calculate even if the question of their stability is ignored.

In summary, the non-inertial forces specified above can be taken into account in many of the simple motions specified in Sec. 1. However, the degree to which such physical variables are involved may vitally affect the stability of the interface involved, i.e., whether perturbations grow or decay. Part II is devoted to the exact analysis of this question by classical perturbation methods.

3. The Five Stages of Mixing.

Although "Taylor instability" had been considered earlier*, the first quantitative correlation of theory with experiment was made in the classic publications of Taylor and Lewis (Refs. 15,12). These concerned Case A; the theoretical analysis ignored surface tension, viscosity, and compressibility.

*Ref. 5, Ch. XI, Sec. 12.

The definitive results concerned growth of sinusoidal perturbations with wave-length λ in a liquid-gas interface, accelerated at a = 30 g - 75 g for a distance of 5 λ - 15 λ . It was concluded that "the instability is made up of the following stages:

"(1) an exponential increase in amplitude as given by the first-order* theory until the amplitude is about 0.4 λ .

"(2) a transition stage during which the amplitude increases from 0.4 to 0.75 λ , and the surface disturbance changes to the form of round-ended columns of air penetrating into the liquid, which form narrow upstanding columns in the interstices;

"(3) a final stage of penetration through the liquid of the air columns at a uniform velocity proportional** to $\sqrt{a - g}$."

Detailed minor comments on the preceding conclusions are made in Secs. 11, 16 and 23. However, there are a few major qualifications which should be made at this point. First, the conclusions refer only to the case $\rho' << \rho$ of very unequal fluid densities ρ' and ρ, when Helmholtz instability is unimportant. Second, they refer only to the case of a single dominant sinusoidal initial perturbation. Third, the scale of the experiments was very limited. Last, the columns were not observed for a distance of very many wave-lengths.

Actually, two further stages may be expected (see Sec. 22):

(4) A stage in which the boundaries of the air columns will

---

*This refers to the "perturbation theory" of Part II.

**See Sec. 17 for a discussion of the constant of proportionality.

deform irregularly under the influence of Helmholtz instability and the growth of vorticity, until

(5) The "mixing zone" separating the two fluids is turbulent, and must be analyzed (like turbulence) by statistical methods.

Unless the preceding observations are kept clearly in mind, a greatly oversimplified physical picture of "Taylor instability" is arrived at--but one which is strongly embedded in the literature on the subject. The present report is concerned almost entirely with stability and laminar mixing, i.e., with Stages (1)-(4). Stage (1) is considered in Part II, Stage (2) in Part IV, and Stages (3) and (4) in Part III.

4. Mathematical Formulation.

In Cases A-C and F, the effects of acceleration and gravity can be interchanged in the problems of Taylor instability and mixing, by the following well-known physical principle.

Elevator Principle.* The effect of an acceleration $a(t)$ relative to the laboratory frame is the same as an apparent gravity $g(t) = -a(t)$, relative to an accelerated frame moving with the fluid.

Thus, if an apparatus is accelerated down with an acceleration a_1, the effect (in the accelerated frame) is to produce an apparent gravity field with intensity $a = a_1 - g$ upwards.

From now on, we shall refer to such a reference frame unless

*J. L. Synge and B. A. Griffith, "Principles of Mechanics", McGraw-Hill, 1942, p. 141.

otherwise specified. We shall let a denote the virtual gravity field to recall the fact that it "really" is an acceleration of the laboratory frame, with a small correction for the earth's gravity field. One advantage of the accelerated reference frame is that the interface undergoes no mean motion in it.

In Helmholtz and Taylor instability and mixing, the most basic parameter is the density ratio ρ'/ρ of the two fluids. Actually, the ratio (Atwood ratio)

$$\alpha = \frac{\rho - \rho'}{\rho + \rho'}, \tag{1}$$

which varies between the limits -1 and 1, is somewhat more convenient mathematically. If the initial conditions involve a fixed wave-length λ, then the ratio of displacement distance to the wave-length,

$$D/\lambda = \frac{1}{2} at^2/\lambda , \tag{2}$$

is also very important (see Sec. 3).

To analyze the role of these and other dimensionless ratios, we shall now give a precise mathematical formulation of the problems of Taylor instability and mixing, in which viscosity and compressibility are neglected.

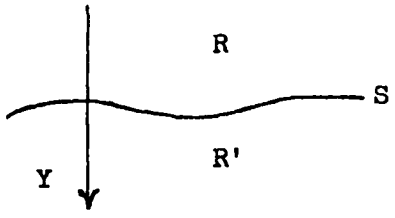

Fig. 1

Suppose space divided into two regions R and R', filled with incompressible, non-viscous fluids of densities ρ and ρ', and separated by an interface S, whose surface tension is T. By the Elevator Principle, we need only consider the case that the fluids are at rest at infinity, but subject to a variable external gravity field g(t). Suppose g(t) points down along the negative y-axis, corresponding to an upward acceleration of an experimental apparatus along the positive y-axis.

The velocity fields $\vec{u}(\vec{x};t)$ and $u'(\vec{x};t)$ in the two fluids (Refs. 11, 3) will then be the gradients of suitable velocity potentials $U(\vec{x};t)$ and $U'(\vec{x};t)$, satisfying

$$\nabla^2 U = 0 \text{ in } R, \quad \nabla^2 U' = 0 \text{ in } R', \tag{3}$$

and the condition of acceleration from rest

$$U(\vec{x};t) = U'(\vec{x};t) = 0 \text{ at } t = 0. \tag{4}$$

Pressure in R is given by the Bernoulli equation

$$p + \frac{1}{2}\rho\nabla U \cdot \nabla U + \rho\partial U/\partial t + \rho g y = C(t) \text{ in } R, \tag{5}$$

and by a similar equation in R'. If $\mathcal{K}(\vec{x})$ denotes the mean curvature at a given point $\vec{x}$ on S, the equation for the pressure jump across S is thus

$$\frac{1}{2}(\rho\nabla U \cdot \nabla U - \rho'\nabla U' \cdot \nabla U') + (\rho\partial U/\partial t - \rho'\partial U'/\partial t') + (\rho - \rho')\, g(t)\, y - T\mathcal{K}(x) = C_1(t) \text{ on } S. \tag{6}$$

Similarly, the equation of continuity is

(6') $\partial U/\partial n = \partial U'/\partial n$ across S.

We thus have a boundary value problem involving the partial differential equations (3), and the boundary conditions (4), (6) and (6'). (We shall not comment on the boundary conditions of rest, or zero velocity, at infinity. We shall also ignore the logical absurdity that $p \downarrow -\infty$ as $y \uparrow \infty$, as this does not seem to cause any essential trouble.)

5. Dimensional Analysis.

In terms of the preceding mathematical formulation, one can give a logical discussion of the applications of dimensional analysis and similarity to the problems of Taylor instability and mixing.

The simplest case is that of purely inertial forces, in which T is supposed negligible in Eq. 6. It is well-known (Ref. 3, p. 97) that inertial hydrodynamics is invariant under arbitrary changes $\vec{x}_1 = \delta \vec{x}$, $t_1 = \epsilon t$ and $\rho_1 = \gamma \rho$ of the length, time, and mass scales. The corresponding effects on velocity-potential and acceleration are evidently $U_1 = (\delta^2/\epsilon) U$, $a_1 = (\delta/\epsilon^2) a$. Substituting in Eqs. 3, 4, 6 and 6', we deduce the following principle valid in the laboratory frame:

Similarity Principle. Let two fluid configurations Σ and Σ_1 be initially similar under the correspondence $\vec{x}_1 = \delta \vec{x}$ and have the same density ratio $\rho'_1/\rho_1 = \rho'/\rho$. Let Σ be accelerated with constant

acceleration a, and Σ_1 with a_1. Then neglecting viscosity, compressibility, and surface tension, the configurations will be similar at corresponding times $t_1 = \sqrt{\alpha a/a_1}\ t$ and $t = \sqrt{\alpha_1/\alpha a}\ t_1$, still with $\vec{x}_1 = \alpha \vec{x}$.

This principle was used by Martin and Price (Ref. 13) in their model studies of the base surge from an atomic bomb.

This implies that initial sinusoidal perturbations of wavelengths λ and λ_1 and equal steepness will develop similarly. If ordinary gravity g is much less than a and a_1, the stage of development will be determined as in Eq. 2 by D/λ, where D is the total displacement.

For other principles of inertial similarity, applicable to the initial stages of motion, see Secs. 6 and 16. We shall now turn to the determination of dimensionless parameters expressing the relative importance of the non-inertial physical variables listed in Sec. 2.

For a sinusoidal interface $y = A \sin(2\pi x/\lambda)$, of wave-length λ and amplitude A, the difference in hydrostatic pressure at trough and crest is $(\rho - \rho')\, aA$, while the difference in pressure jumps due to surface tension is $8\pi^2 AT/\lambda^2$ (the curvatures are $4\pi^2 A/\lambda^2$). Hence, the relative importance of surface tension evidently corresponds to the modified Weber number

$$\tau = 8\pi^2 T/(\rho - \rho')\, a\lambda^2. \tag{7}$$

The effect of viscosity increases with time, since the associated dif-

fusion travels a distance of $\sqrt{\nu t}$ in time t; hence it is indicated by either

(8) $$R = \nu t/\lambda^2 \text{ or } R_1 = \nu t/\lambda D = 2\nu/\lambda a t.$$

As regards compressibility, the change in density per wave-length is approximately

$$\Delta\rho = \Delta p/c^2 = \rho a \lambda/c^2 \qquad (c = \text{sound velocity})$$

Hence, its importance is roughly measured by

(9) $$\rho a \lambda/c^2(\rho - \rho') \text{ or } \lambda a/c^2\alpha \qquad \text{(cf. Eq. 1)}$$

(The ratio $\lambda a/cc'\alpha$ would be more symmetrical.)

Some further remarks on similarity are made in Appendix A.

6. Initial Acceleration.

As little is known about the role played by compressibility and viscosity in Taylor instability, we shall turn back to the inertial model and in particular to the initial phase, Stage (1), of Helmholtz and Taylor instability. Here, two classical mathematical methods can be used.

The first is Kelvin's Theory (1871) of the perturbations of a plane interface, and its extension to spherical and cylindrical bubbles by Penney and Price (1942)*. This theory will be reviewed and extended in Part II, and requires no further introductory comments.

*British Report SW-27 (1942); see R. H. Cole, "Underwater Explosions", Princeton, 1948, p. 311.

The second is the case of the initial acceleration, at $t = 0$, of an interface of arbitrary shape. In this case, if $\partial U/\partial t$ and $\partial U'/\partial t$ are denoted by A and A', we can eliminate $p - \rho gy$, $p' - \rho' gy'$ by Eq. 5, to give the equations $\nabla^2 A = \nabla^2 A' = 0$ and

$$\left.\begin{aligned} \rho A = \rho' A' = \kappa y \qquad (10) \\ \partial A/\partial n = \partial A'/\partial n \qquad (10') \end{aligned}\right\} \text{ on S}$$

But these equations define various well-known problems of mathematical physics, including those of magnetostatic and electrostatic polarization of an inhomogeneous medium in a uniform field. The case that R is bounded (see Fig. 2) has received the most attention in the literature, and was first treated by Poisson in 1825.

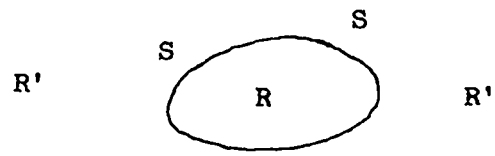

Fig. 2

We shall show in Part IV that the problem of Taylor mixing can be reduced to a continuum of boundary value problems of the type of Eqs. 10 and 10', and shall discuss the problem of their effective solution on high-speed computing machines. For the present, we shall merely recall some interesting known facts, referring the reader to Appendix B for references and further comments, and to the forthcoming

Harvard Doctoral Thesis of James Howland* for an exhaustive treatment of the subject.

One interesting fact is that the initial acceleration of spherical and ellipsoidal fluid globules is the same as if they were rigid. The internal "induced field" is uniform. Moreover, there are no other bounded shapes having this rigidity property. (Paraboloids presumably do, but are unbounded.)

Again, the system (Eqs. 10 and 10') is equivalent to a Fredholm integral equation involving the parameter α of Eq. 1, and a distribution** on S as the unknown function. It follows that each interfacial configuration and external gravitational field (acceleration in the laboratory frame) is consistent with just one acceleration field. Thus our "inertial" formulation of the instantaneous acceleration field problem is "well set", in the sense of Hadamard.

Similar remarks apply to Case B of impulsive motion, in view of the following:

Impulsive Motion Principle. Let $A(\vec{x})$ be the initial acceleration potential induced, for a given configuration Σ and density ration ρ'/ρ, by a unit acceleration at infinity. Then, as $T \longrightarrow 0$, the velocity potential associated with $\int_0^T a(t)\,dt = V$ tends to $U(\vec{x}) = V\,A(\vec{x})$.

---

*This is sponsored by the Los Alamos Scientific Laboratory under Subcontract SC-7 and should be completed in June 1955.

**Single or double layer, in the sense of potential theory (See Ref. 10, pp. 160-72).

7. Experimental Data.

Taylor and Lewis (Refs. 15, 12) showed conclusively that Kelvin's perturbation theory, with only inertial forces (Sec. 2) considered, gave an adequate quantitative explanation of their data in Stage (1), for the case of an initially sinusoidal perturbation, with $\rho'/\rho \ll 1$. In this case, they were also able to explain Stage (3). Here, the rate of bubble rise is about that which would be expected from ordinary bubble rise (Sec. 17). More recent data by Allred (Ref. 1) partially supports the idea that formulas similar to those obtained by Taylor and Lewis are applicable without the hypothesis $\rho' << \rho$. Thus various predictions of the amount of Taylor mixing have been based on a simple scaling up of Lewis' data, using the Similarity Principle of Sec. 5.

More recent work has brought out both improvements in the Taylor-Lewis analysis and a clearer understanding of the limitations on its applicability, due to the roles of surface tension and Helmholtz instability, which were largely ignored by Taylor and Lewis. This work will be critically reviewed, and compared with fresh theoretical and experimental data, in Part III.

Stages (2) and (3) can also be analyzed in principle, by an attempt to solve numerically the initial value problem of Sec. 4. This attack is very promising but has not been successfully carried through yet. Past efforts and future prospects in this direction will be critically reviewed in Part IV.

When we come to Stages (4) and (5), it must be admitted that very little is known, either theoretically or experimentally. Moreover the methods which have been applied to Stages (2) and (3), even with the use of high-speed computing machines, do not seem promising. All that can be reliably guessed is, that the asymptotic formulas of Stage (3) probably overestimate the depth of interpenetration. Also, the duration of Stage (4) can be estimated.

The analysis of Stage (5) requires statistical methods and will be deferred until a later report.

II. PERTURBATION THEORY

8. Kelvin's Formulas.

As already observed (Sec. 1), a plane interface is clearly in equilibrium under any acceleration $\tilde{a}(t)$ in any uniform gravity field, provided both are normal to its surface. Using the Elevator Principle of Sec. 4 to combine $\tilde{a}(t)$ and gravity into a single "apparent gravity", $g(t) = g - \tilde{a}(t) = -a(t)$, the equations of Sec. 5 are satisfied by

$$(11) \qquad p = -\rho a(t) \left[y - y(t)\right], \quad p' = -\rho' a(t) \left[y - y(t)\right],$$

where $y - y(t)$ expresses position in the accelerated frame moving with the fluid, so that $y(t) = \int v(t)\, dt$, where $v(t) = \int \tilde{a}(t)\, dt$. The preceding ideal flow involves pressures which become positively and negatively infinite at infinity, but it gives a reasonable picture over a large region of space.

Equation 11 brings out the equivalence (with reversed signs) of acceleration at infinity and a uniform gravitational field. In a frame accelerated with the fluid, the problem is that of a fluid, motionless at infinity, in an external gravity field $\left[g - a(t)\right]\vec{j}$.

One can superpose on any normally accelerated flow, whose pressure satisfies Eq. 11 , arbitrary constant velocities u and u' parallel to the interface, without affecting the equilibrium. Most

important is Case A of a constant gravity field, which has been investigated mathematically by Kelvin (1871), Rayleigh (1879) and others*; we shall summarize the results of the analysis. The mathematical analysis assumes two perfect (incompressible non-viscous) fluids, with an interfacial tension $T \geq 0$. The "gravity" $g - \tilde{a} = -a$ is assumed constant, but otherwise arbitrary. The effect of viscosity is harder to treat (see Ref. 2).

Moving axes can be introduced, relative to which the velocities u and u' of the two fluids relative to these axes are parallel to the x-axis and satisfy $\rho u + \rho' u' = 0$. A small sinusoidal perturbation $y = A(k,t) \sin kx$ of the interface, parallel to the x-axis and with wave number k, then has an amplitude $A = A(k,t)$ which satisfies the ordinary differential equation

(12) $$\ddot{A} = S(k)\, A, \text{ where}$$

(12') $$S(k) = \frac{\rho\rho' k^2}{(\rho + \rho')^2} (u' - u)^2 + \frac{\rho - \rho'}{\rho + \rho'} (a - g)k - \frac{Tk^3}{(\rho + \rho')} .$$

From Eqs. 12 and 12', a number of qualitative inferences can be drawn immediately.

I. The condition for stability is that $S(k) < 0$ for all $k > 0$. (The proof is an obvious application of Fourier analysis.)

---

*Lamb, Sec. 232, 234 and 268, and references given there. Kelvin applied the formulas to the generation of waves by wind (cf. Sec. 5); Rayleigh, to jet instability and flapping flags.

II. The relative tangential velocity $|u - u'|$ is always a destabilizing factor. Instability due dominantly to this cause is called Helmholtz instability*.

III. Acceleration $a > 0$ from the denser towards the lighter fluid exerts a stabilizing tendency; acceleration from a light towards a dense fluid exerts a destabilizing tendency. Instability due primarily to this cause is called Taylor instability.

IV. Surface tension exerts a stabilizing tendency on the shorter ripples, and stabilizes sufficiently short ripples, thus keeping the interface from getting too irregular.**

Looking at the magnitude of the coefficients in Eq. 12', we see also that

V. Helmholtz instability is small if $\rho' << \rho$ (or $\rho << \rho'$), while Taylor instability is small if ρ' and ρ are nearly equal.

9. Most Unstable Wave-Length.

A more careful scrutiny of Eqs. 12 and 12' gives a quantative idea of the rate of exponential growth (or decay) of perturbations.

The simplest case is that of an initially sinusoidal perturbation, with wave-length $\lambda = 2\pi/k$. If there is no tangential motion, so that $u = u'$, and if surface tension is ignored, we get Taylor's elementary solution

---

*Because it was first stressed by Helmholtz (Ref. 9) in 1868.

**This was first noted in the present context by R. Bellman and R. H. Pennington (Ref. 2). See also (Ref. 4, pp. 9-10).

(13a) $A = A_o \cosh \nu t$, where $\nu = \sqrt{\alpha\, ak}$ (cf. Eq. 1).

This simple formula adequately explains Lewis' observations of Stage (1), for the case of an initial sinusoidal perturbation; $\alpha = 1$, nearly, since $\rho' \ll \rho = 1$.

We next consider the case of a general initial perturbation, with Fourier components from a continuum of frequencies. In this case, each Fourier component will have its own rate of growth. Under the simplifying hypotheses leading to Eq. 13a, the rate of exponential growth will tend to infinity with k. This conclusion shows* that Kelvin's perturbation equations leading to Eqs. 12 and 12' do not have any solution in general -- they involve a paradox in the general case!

This paradox can be resolved in either of two ways. First, one can observe that the assumptions underlying the derivation of perturbation equations break down, as soon as the perturbation amplitudes cease to be infinitesimal. This resolves the paradox, but it leaves one without a theory (see also Sec. 21).

A more positive approach is achieved by taking into account the effect of surface tension. If the fact that $T > 0$ is recognized, still with $u = u'$, we get instead of Eq. 13a, the formula

(13b) $A = A_o \cosh \nu t$, where $\nu^2 = \alpha\, ak - Tk^3/(\rho + \rho')$

We see immediately that $\nu^2 < 0$ if $k^2 > \alpha\, a(\rho + \rho')/T$. Hence wave-

*G. Birkhoff, Journal of S.I.A.M. (1954)

lengths λ shorter than the critical wave-length

(13c) $$\lambda_c = 2\pi\sqrt{T/\alpha a(\rho + \rho')} = 2\pi\sqrt{T/a(\rho - \rho')}$$

are stable. Alternatively, referring to Eq. 4, the criterion for stability is that the Weber number $\tau > 2$.

It is equally clear that the most unstable wave-length λ_α, having the fastest exponential growth, corresponds to the case $d(\nu^2)/dk = 0$, or to

(13d) $$\lambda_d = \sqrt{3}\,\lambda_c \simeq 10.7\sqrt{T/a(\rho - \rho')}.$$

In the case of an air-water interface, with $T \simeq 80$ in cgs units and $\tilde{a} = ng$ measured in units of g, this becomes $\lambda_d \simeq 3\sqrt{n-1}$ cm. Theoretically, since exponential growth dominates ratios of initial amplitudes, one would expect wave-lengths near λ_d to be the first to achieve finite (observable) amplitude, in the case of a random, non-periodic initial disturbance. Hence λ_d may also be expected to be the dominant wave-length. This expectation is partially confirmed in Ref. 12, Plate 8, which shows 15-30 protuberances in Stage (1), giving $\lambda \simeq 0.5$ cm for $n \simeq 130$ effects. Modifications of Eqs. 13b and 13d, taking account of viscosity effects, may be found in Ref. 2.

We shall now pause to examine critically some experimental evidence, which should caution one against accepting the implications of Eqs. 12 and 12' too readily.

10. Experimental Data

First, we shall see how the experiments of Lewis, Allred, and Duff fit the preceding theoretical analysis of Stage (1) of Taylor instability. In order to make such a comparison, it will be necessary to mention a few of the many experimental difficulties involved in making "clean" experiments. As already stated, the case of an air-water (or liquid-gas) interface with an initial sinusoidal perturbation and a $\simeq$ 100 g fits Taylor's simplified formula (Eq. 13a) very well, and no further comment on this case seems necessary.

The case of a liquid-liquid interface is considerably more difficult. With many liquids, there is a gradual thickening of the interface, and so Kelvin's formulas are not applicable*. Allred found that, in those cases where a sharp meniscus was observable, the observed rate of growth of an initially sinusoidal perturbation was somewhat less than that predicted by Eq. 13b, with a fair amount of experimental scatter**. His confirmation of Eq. 13c was also satisfactory (Ref. 1, Fig. 4.3). In the case of water-n-heptane, where a sharp meniscus was observed (Ref. 1, p. 21), the confirmation was especially good. In other cases, the experimental λ_c was about twice that predicted by

*For this case, see Appendix C. Lewis was not successful in getting clean-cut results with a liquid-liquid interface; see his Plate 10.

**See Ref. 1, Fig. 4.2B. The author believes that Allred's "experimental" α may be about 15% too low, because of his use (see his Fig. 4.12) of Log μ plots instead of $\text{Cosh}^{-1}\mu$ plots. Thus he loses a growth-factor of two, in a total growth by a factor of 10. This would also explain why his experimental points fall to the right of his straight line, in the 8-25 Frame region.

Eq. 13c. In Appendix C, this will be explained in terms of diffusion of the interface.

Interesting observations of liquid-liquid and gas-gas interface instability, with a = g, have also been made by Duff and Knight (Ref. 7). For good reasons not relevant to the present discussion, the interface was stabilized by a thin plate before the experiment. As the plate was drawn aside, a periodic wake was generated* which seemed to have more influence on the dominant wave-length than Eq. 13d. Hence the experiments shed little light on Stage (1) of the development of Taylor instability.

In summary, the formulas of Sec. 11 seem to explain the observed facts in Stage (1), for sinusoidal and non-sinusoidal initial perturbations alike, provided: (1) surface tension is taken into account, (2) the interface is initially a surface of discontinuity, (3) the experiment is "clean" in the sense that wall effects and other extraneous influences do not act on the region under observation.

Digression. The applicability of Eqs. 12 and 12' to real Taylor instability is a question logically analogous to their applicability to real Helmholtz instability (e.g., the generation of waves by wind). We shall briefly review the facts for the sake of comparison.

Theoretically**, a wind velocity of 640 cm/sec is required to

*See S. B. Hollingdale, Phil. Mag. 29 (1940),209-57; C.A. Gongwer,J.appl. mech. 19 (1952),432-8. The subject will be reviewed in Ch.XIII of Ref. 5.

**All numerical values are taken from the classic paper of H. Jeffreys, Proc. Roy. Soc. Lond. (A) 107 (1924) 189-205. Kelvin (op. cit., p. 81) already stressed the importance of the difference in pressure between the windward and leeward sides of real waves.

produce waves; the corresponding wave-length is $\lambda = 1.8$ cm, and the wave-velocity, 0.8 cm/sec. Experimentally, waves are formed at a wind velocity of 110 cm/sec; their length is 6-8 cm, and they travel at 30 cm/sec. This discrepancy is commonly ascribed to the fact that airflow separates at the crest of the wave, so that there is underpressure on the lee side. However, the whole subject is complicated by atmospheric (and oceanic) turbulence, which produce (through eddy viscosity) substantial variations in the mean velocity with distance from the interface*.

11. Impulsive Acceleration.

The case of "impulsive" acceleration from rest (Case B in the scheme of Sec. 1) can also be treated using Kelvin's formulas (Eqs. 12 and 12'). We suppose a total velocity $v = \int a(t)\, dt$ to be imparted in time t, during which the interface moves through a distance d of about $vt/2$. In this case, clearly T, g, and (u'-u) will be especially negligible.

To treat this case, we rewrite Eqs. 12 and 12' as

$$\dot{dA} = A \alpha k\, a(t)\, dt. \tag{14}$$

For sufficiently "long" waves, with very small k, clearly A will be nearly constant during the impulse, and so we will have

$$\dot{A} = \alpha k\, v\, A \qquad \text{for "long" waves.} \tag{14a}$$

*This aspect was stressed by Jeffreys and earlier by Rayleigh, Proc. Lond. Math. Soc. 11 (1880) 57-70. See also C. Eckart, J. appl. phys. 24 (1953), 1485-94.

The growth of A will be bounded by $\dot{A}t$; hence a wave will be "long" if $\dot{A}t \ll A$, or $\alpha k v/T \ll 1$. In other words,

(14a') a wave is "long" if $\lambda \gg 4 \alpha d$.

Again, extremely "short" waves will grow exponentially after a brief initial phase, and will even enter Stage (3) of "spikes" and "bubbles". Thus, in the case of a constant "step wave" acceleration v/t, the total amplification factor will be $\cosh (\sqrt{\alpha a k t}) = \cosh \sqrt{\alpha k v t}$, by Eq. 13a. Hence, a wave is "short" if

(14b) $$\lambda \ll 2\pi\alpha v t = 4\pi\alpha d.$$

Such short waves will have a velocity of rise bounded by $\sqrt{a\lambda}$ (see Part III); hence their total rise will be bounded by $\sqrt{\lambda a}\, t = \sqrt{\lambda v t} \doteq \sqrt{\lambda d}$. In view of Eq. 14b, λ is bounded by $4\alpha d$, however.

We conclude that the maximum spike fall A observed will have the order of $2d\sqrt{\alpha}$, and will be associated with wave-lengths of the order of $4\alpha d$, and with upward velocity $2\sqrt{\alpha}\, v$.

Allred has observed impulsive accelerations*, with $\alpha = 0.2$, $a = 200$ g and $t = 0.001$ sec, approximately. Hence $v = 200$ cm/sec, $d = 0.2$ cm, and $\alpha d = 0.4$ mm. The maximum spike fall does seem to be of the order of $\sqrt{\alpha}\, d = 1$ mm. The average space between spikes seems to be about 3 mm, which is considerably more than the predicted 1 mm, however, and the data are complicated by the occurrence of cavitation which Allred attributed to transverse vibrations of the side walls

*See Ref. 1, Chap. V, where much of the preceding analysis is presented in another form, on pp. 24-25.

(Ref. 1, p. 26). Hence the rough experimental confirmation of the calculations made above cannot be regarded as conclusive.

12. Spherical Cavities.

The radial motion of a spherical cavity admits of fewer degrees of freedom, because (1) a cavity of changing radius must necessarily be compressible, and (2) Helmholtz instability cannot be included within the framework of perturbation theory. Thus, in searching for analogs of Kelvin's formulas Eqs. 12 and 12', one is restricted necessarily to the cases $u = u' = 0$ and $\alpha = 1$. Within these limitations, and the neglect of gravity, one can, however, develop perturbation formulas for "Taylor instability" analogous to Eqs. 11 and 11'.

Such formulas, with surface tension also neglected, were derived during World War II by Penney and Price*, and applied to underwater explosions. Suppose the mean cavity radius given as a function $b(t)$ of time, and let the interface be expressed in spherical coordinates by

$$r = b(t) + \sum_{h=1}^{\infty} b_h(t)\, P_h(\cos \phi), \tag{15}$$

in terms of Legendre polynomials. Supposing the $b_h(t)$ small, and neglecting gravity and surface tension, the condition of constant internal pressure gives

$$b\ddot{b}_h + 3\dot{b}\dot{b}_h - (h - 1)\ddot{b}b_n = 0. \tag{16}$$

*British Report SW-27 (1942); see R. H. Cole, "Underwater explosions", Princeton, 1948, p. 311.

The same formula applies to any surface harmonic of order h; we omit the derivation.

For a differential equation of the form

$$\ddot{x} + p(t)\,\dot{x} + q(t)\,x = 0 \tag{17}$$

to be stable, we have the criterion*

$$q > 0, \qquad 2pq + \dot{q} > 0. \tag{17'}$$

Substituting Eq. 16 in Eqs. 17 and 17', we obtain the stability criteria

$$-\ddot{b} > 0 \qquad \text{and} \qquad b\dddot{b} + 5\,\dot{b}\,\ddot{b} > 0. \tag{18}$$

(The second criterion can also be interpreted as meaning that $b^5\ddot{b}$ must be an increasing function.)

The condition $\ddot{b} < 0$ evidently amounts to Taylor's stability criterion (Sec. 1) that the acceleration be from the denser towards the lighter medium. The second condition amounts roughly to requiring positive damping; if $\dddot{b} = 0$, it would be equivalent to $-\dot{b} > 0$ in Eq. 16.

Further consideration of Eq. 18 shows that a cavity collapsing inertially to a point is unstable**, even though the acceleration is always centripetal. The amplitude of perturbations grows like $b^{-1/4}$ as $b \downarrow 0$, if viscosity is neglected.

---

*See M. S. Plesset, J. appl. phys. 25 (1954); 96-98, where surface tension (and general α!) are admitted. Caution. Plesset's "stability criteria" are erroneous. See G. Birkhoff (note to appear in Quar. Appl. Math.) for Eq. 17'.

**For details, see G. Birkhoff, Quar. Appl. Math. 12 (1954), 306-309.

The effect of viscosity on spherical (unperturbed) cavity collapse has been considered by H. Poritsky and S. S. Shu*. Since the rate of strain is proportional to $\dot{r}/r = \dot{V}/r^3$, if V denotes cavity volume, and the rate of strain equals the rate of viscous work per unit volume, the rate of viscous work is $\dot{V}\, dr/r$, which becomes infinite as the cavity radius tends to zero.

13. Cylindrical Cavities; Periodic Oscillations.

The results of Sec. 12 can be generalized in various ways.

Thus, one can investigate the stability of a cylindrical cavity. Instead of Eq. 15, one writes

(15a) $$r = b(t) + \sum_{h=1}^{\infty} b_h(t) \cos h\,\theta.$$

Instead of Eq. 16, one gets

(16a) $$b\,\ddot{b}_h + 2\,\dot{b}\,\dot{b}_h - (h-1)\,\ddot{b}\,b_n = 0$$

Instead of Eq. 18, one gets

(18a) $$-\ddot{b} > 0 \qquad \text{and} \qquad b\dddot{b} + 3\,\dot{b}\,\ddot{b} > 0.$$

The case of a cavity collapsing to a point is neutrally stable, to a first approximation. (However, to a higher approximation, perturbation amplitudes may grow logarithmically).

Again, in both the spherical and cylindrical case, one can treat the case of several concentric shells of different densities.

---

*

This will be done in Appendix C.

Case C of periodic oscillations has also attracted interest in various connections.

Thus, the case of a plane gas-water interface arises in the case of a Humphreys pump*, whose efficiency is impaired by the resulting Taylor instability. An interesting mathematical discussion, applicable to Stage (1) of this case, has recently been given by Ursell and Benjamin**. In particular, it is explained why the frequency of the standing waves may be half that of the impressed oscillations. The theory is based on that of the Mathieu equation.

The case of the oscillating gas bubble formed by an underwater explosion is of even greater importance, while the stability of periodically oscillating cavitation bubbles has been considered in the references of Sec. 12.

*See Gibson, "Hydraulics", Art. 217; W. G. Noack, Zeits. VDl 57 (1913), 885-92; Prof. J. Ackeret called this instance of Taylor instability to the author's attention.

**Proc. Roy. Soc. A225 (1954), 505-15.

III. ROUND-ENDED BUBBLES

14. Taylor's Analysis.

Part III of this report will concern the analytical theory of Stages (2), (3), and (4) of Taylor instability. Taylor's ideas have exerted such a great influence on subsequent work that we shall begin by commenting in detail on his analysis, of which Lewis' own summary has already been repeated in part verbatim in Sec. 3.

It will be recalled that Taylor and Lewis analyzed the case of an initially sinusoidal perturbation of wave-length λ, with fluids of densities $\rho' << \rho$, so that $\alpha = 1$ in Eq. 1. In this case, the transition from Stage (1) through Stage (2) into Stage (3) was very clear. Stage (3) (called the "final" stage by Taylor and Lewis, Sec. 3) was regarded by them as analogous to the case of a "cylindrical bubble" (Sec. 15), or bubble rising at constant velocity in a cylindrical tube of radius a. For such a bubble, Taylor and Davies* calculated rate of rise to be $v = 0.48 \sqrt{g\,a}$. By analogy, the rate of rise of a two-dimensional bubble of diameter λ (see Fig. 3) should be given by a formula of the $v = C \sqrt{g\,\lambda}$, as also follows directly from dimensional analysis and similarity. The numerical value of C will be discussed in Sec. 15.

*R. M. Davies and Sir G. Taylor, Proc. Roy. Soc. A200 (1950), 375-90.

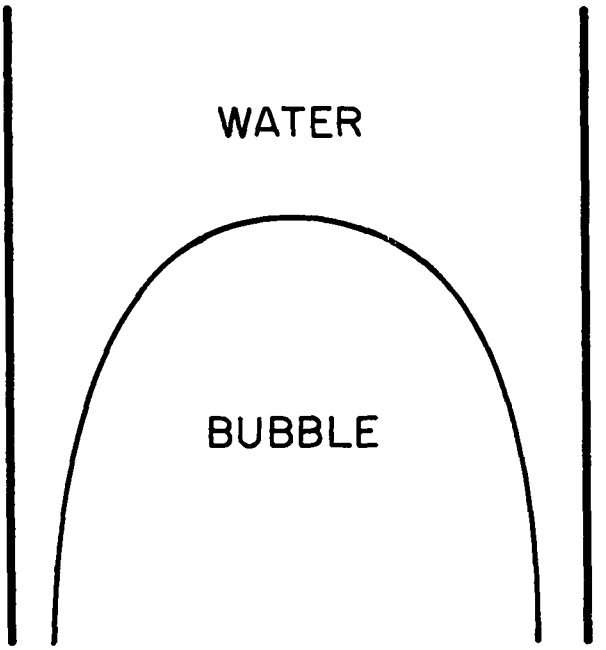

Fig. 3

The "narrow upstanding columns in the interstices" between the bubbles were asserted by Taylor and Lewis to fall freely under gravity in Stage (3), so that their depth of penetration was given by a formula $\delta = \frac{1}{2} a (t - t_1)^2$.

Even if Stage (3) is regarded as the "final stage" of Taylor instability (cf. Sec. 3), several questions are left unanswered by the preceding analysis. What is the duration of the transition from Stage (2) to Stage (3)? Can this be predicted approximately on a strictly "inertial" basis, without considering the effects of surface tension, viscosity, etc.? What if the initial perturbations are not periodic corrugations? What about the general case $\alpha \neq 1$ of comparable densities? What is the interfacial configuration in Stage (3) for three-dimensional disturbances--e.g., does one have bubbles separated by "spikes" or "curtains"? These questions will be treated in Secs. 16-19.

Furthermore, an estimate of the duration of Stage (3) is desirable. Such an estimate will be given in Sec. 21.

15. Bubble Rise Velocity.

Axially symmetric bubbles rising under gravity in a cylindrical tube have been studied by Gibson and Dumitrescu*, as well as by Davies and Taylor. For a tube of diameter d, in the range $1 \text{ cm} < d < 10 \text{ cm}$, the following empirical formulas are approximately correct:

---

*A. H. Gibson, Phil. Mag. 26 (1913), 952-65; D. T. Dumitrescu, Zeits. ang. Math. Mech. 23 (1943), 139-49.

(19) $v = 0.32 \sqrt{g\,d}$, $R = 0.35\,d$, $v = (2/3)\sqrt{g\,R}$, if $\alpha = 1$,

where R is the radius of curvature of the bubble vertex. For $d < 1$ cm, surface tension becomes very important; the range $d > 10$ cm has not been explored experimentally.

In terms of the Weber number $\tau = 2\pi^2 T/(\rho - \rho')\,a\,d^2$ (Eq. 7, with $\lambda = 2d$), surface tension thus becomes important when $\tau > 1.5$, as might be expected (cf. Sec. 9). To correct for surface tension, and allow for variable α, the following rough argument may be used, analogous to that used by Davies and Taylor. The argument ignores viscosity effects.

In Fig. 2, the inside of the bubble is supposed to rise rigidly; the outside to flow down around the bubble. The difference between the static vertical pressure gradients inside and outside the bubble is $(\rho - \rho')\,a$ (we replace g by a); the vertical gradient of the pressure jump $2T/R = 2kT$ due to curvature (See Ref. 11, p. 456) is $2\,T/R^2$, where R is the radius of curvature of the bubble tip, as in Eq. 19. By analogy with flow around a sphere, the pressure gradient in the flowing liquid may be estimated as about $9\rho v^2/4\,R$. Hence, the equation

$$9\rho v^2/4\,R = (\rho - \rho')\,a - 2\,T/R^2$$

expresses (roughly) the condition of pressure continuity across the interface. Solving, we get

(19a) $$v = \frac{2}{3}\sqrt{\left(\frac{\rho - \rho'}{\rho}\right) a R \left(1 - \frac{4}{\tau}\right)}, \tau = 2T/(\rho - \rho') a R^2$$

(cf. Eq. 7), where $a = a_1 - g$ is the net field, as in Sec. 4. This agrees with the third formula of Eq. 19.

However, one should also remember that the bubbles which have been observed experimentally (see Refs. 1, 7 and 12) in connection with Taylor instability are two-dimensional. The two-dimensional analog of the displayed equation above (Eq. 19a) is

$$4\rho v^2/R = (\rho - \rho') a - T/R^2$$

Hence, a two-dimensional bubble should rise with velocity

(19b) $$v = \frac{1}{2}\sqrt{\left(\frac{\rho - \rho'}{\rho}\right) a R \left(1 - \frac{2}{\tau}\right)}.$$

In the case of negligible ρ', τ treated by Lewis, this should simplify to $v \simeq 0.5\sqrt{a R} \simeq 0.3\sqrt{a d}$, using Eq. 19 to estimate d. Experimentally, Lewis found $v \simeq 1.1\sqrt{a R}$; the data are in Ref. 12, Fig. 20.

An exact mathematical theory of two-dimensional bubbles is given in Appendix D (written jointly with David Carter). It gives the estimate

(19c) $$v_o = 0.25\sqrt{a d}, \qquad \text{(experimentally, } v_o = 0.285\sqrt{ad}\text{)}$$

carried to a first rough approximation, confirming Eq. 19b. The larger values (by a factor of two) found by Lewis may be partly explained by the fact that, in Stage (3) of his experiments, a considerable fraction of the water is included in the freely falling spikes, so that the

acceleration of the rest considerably exceeds the initial acceleration.

16. Duration of Stage (2).

The Similarity Principle of Sec. 5 leads us to expect Stages (1) and (2) to follow a growth law of a form like

$$\ddot{A} = \alpha a f(A/\lambda), \tag{20}$$

provided surface tension, viscosity, and $|u' - u|$ are negligible. In Stage (1), by Eq. 12', $f(A/\lambda) = Ak = 2\pi A/\lambda$. Empirically (Ref. 12, p. 94), Stage (1) has been said to hold as long as $A/\lambda < 0.4$, and Stage (2) while $0.4 < A/\lambda < 0.8$, provided $\rho' << \rho$.

By the Similarity Principle of Sec. 5 also, if inertial forces are dominant, the duration T_2 of Stage (2) should satisfy $T_2 = C\sqrt{\lambda/a\alpha}$. Empirically, by Ref. 12, Fig. 19, assuming $d = 3R$, $.006 \simeq C \simeq \sqrt{6/118\ g}$; hence

$$T_2 \simeq 0.85\sqrt{\lambda/a\alpha} \quad \text{very roughly, if } \rho' << \rho. \tag{21}$$

The duration T_1 of Stage (1) is of the same order of magnitude.

We shall see, in Sec. 19, that a clearcut definition of Stage (3) is difficult when $\alpha < 0.5$, say. Moreover, at least in Stage (2), we have $f(A/\lambda, \alpha)$ instead of $f(A/\lambda)$ in Eq. 20.

17. Simplified Analytical Models.

Interesting attempts to deduce the development of Taylor instability from assumed simplified analytical models have been made by Fermi (Ref. 8) and by Layzer*. It is instructive to review these models

*D. Layzer, "On the development of Taylor instability". Report PNJ-LA-3, 1952.

briefly here; a systematic discussion of this type of theoretical approach will be given in Part IV. Both authors assumed $\rho' = 0$ in the lower fluid.

Fermi supposed the interface S constrained to consist of two horizontal and one vertical segment, as in Fig. 4a. The constraints

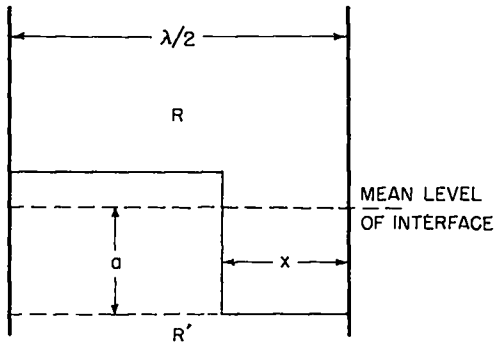

Fig. 4a

being supposed workless, a Lagrangian system with two degrees of freedom is defined, say x and a. The potential energy V and kinetic energy T have the form

(22) $$V = -a^2 x/2(1 - x), \text{ and}$$

(22') $$T = \frac{1}{2} (T_{11} \dot{x}^2 + 2 T_{12} \dot{x} \dot{a} + T_{22} \dot{a}^2).$$

The $T_{ij} = T_{ij}(x,a)$ can presumably be expressed exactly as elliptic integrals. Using approximate evaluations, Fermi integrated Lagrange's equations

$$d(\partial T/\partial x)/dt = \partial(T-V)/\partial x, \; d(\partial T/\partial a)/dt = \partial(T-V)/\partial a$$

numerically for the case $\rho' = 0$. According to the calculations,

Stage (1) ended when $A/\lambda = 0.03$, approximately; the protruding "spike" then got rapidly narrower, falling with an asymptotic velocity $8\,gt/7$, instead of the correct gt. The "bubble" rose with an asymptotic velocity $0.06/\sqrt{t}$; this disagrees badly with Eq. 19.

David Judd* tried replacing the configuration of Fig. 4a with that of Fig. 4b, and came out with worse results:

$$v \simeq 49\, gt^2/19, \quad x \simeq c\, t^{-16/7}.$$

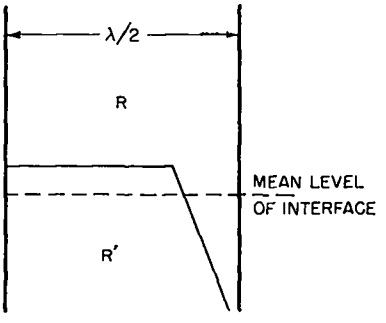

Fig. 4b

Layzer's models are of a quite different type. The admitted fluid configurations depend on a single parameter $q = q(t)$. The velocity field is assumed always proportional to a fixed velocity field, so that the streamlines are time-independent. By inspection of Eqs. 24 and 24a, one sees that they are also all congruent under vertical translations.

Specifically, he assumes in the plane case

$$(23) \qquad -U = \dot{q}\, e^{-y} \cos x, \quad \text{or} \quad \dot{y} = \dot{q}\, e^{-y} \cos x, \quad \dot{x} = \dot{q}\, e^{-y} \sin x.$$

The flow defined by Eq. 23 fills the strip $-\pi/2 < x < \pi/2$, and its wave-

*Letter dated July 10, 1952.

length $\lambda = 2\pi$. The streamlines are sketched in Fig. 5; they are given by

(24) $$e^{y-c} = \sin x.$$

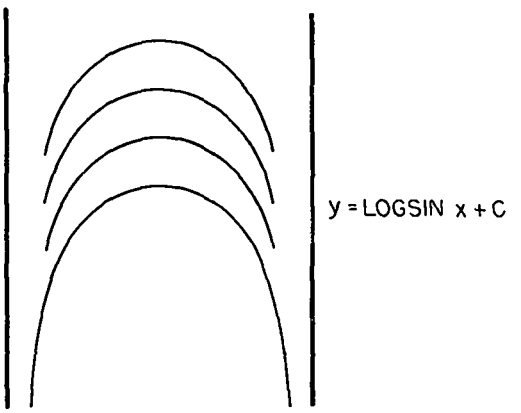

Fig. 5

In the axially symmetric case, Layzer assumes similarly

(23a) $$-U = \dot{q}\, e^{-z}\, J_o(r), \quad \text{or} \quad \dot{z} = \dot{q}\, e^{-z}\, J_o(r), \quad \dot{r} = \dot{q}\, e^{-z}\, J_1(r).$$

Correspondingly, the streamlines are given by

(24a) $$e^{z-c} = r\, J_1(r).$$

The radius of the tube is β_1, the first zero of $J_1(r)$.

In both cases, the behavior at the upper end of the tube agrees asymptotically with what one would get vrom an exact theory. Again, one can express the Davies-Taylor condition of pressure equilibrium at the bubble vertex (See Sec. 15) in terms of q(t). The analog of Eq. 19 is a second-order differential equation in q(t), derived in Appendix E, which agrees with the results obtained in Part II during Stage (1). In Stage (3), it agrees quite well with the results

(Eqs. 19 to 19b) of Davies and Taylor* and Dumitrescu**. Layzer's calculations give $v = \sqrt{gd/2\beta_1} \simeq .35\sqrt{gd}$ and $R = 2d/\beta_1 \simeq .52\ d$ instead of $v = .32\sqrt{gd}$ and $R = .35\ d$. In the plane case, $R = 3d/2\pi$ and $v = 0.4\sqrt{gd} \simeq .58\sqrt{gR}$, instead of $v \simeq 0.5\sqrt{gR}$. One may, therefore, expect the model to give a fair representation of the rate of bubble rise throughout the entire motion.

Unfortunately, the model gives a very poor representation of the speed of fall of "spikes". According to the model, the spikes would extend to infinity when the relative amplitude was only 0.2 in the axially symmetric case, and only 0.11 in the plane case. For the same reason, if the condition of pressure equilibrium at the vertex used by Layzer were replaced by the equation

$$d(dT/dq)/dt \doteq \partial(T - V)/\partial q$$

of energy conservation, a very poor approximation would result, except in Stage (1). Hence, Layzer's model cannot be described as representing what would happen if a flexible diaphragm were inserted at the interface, free to move according to the degree of freedom of motion allowed.

The formulas justifying the preceding statements will be found in Appendix E.

---

*R.M.Davies and Sir G. Taylor, Proc. Roy. Soc. A200 (1950), 375-90.

**D.T.Dumitrescu, Zeits. ang. Math. Mech. 23 (1943), 139-49.

18. Dominant Wave-Length.

From formulas like Eqs. 18 and 19 for the rate of bubble rise, it is clear that the larger bubbles will "eat up" the smaller. This is also evident experimentally (Ref. 12, Figs. 5-8). Moreover, it probably explains the stability of the "cylindrical bubbles" of Sec. 15: smaller competitors of the main bubble drop behind and are absorbed in it.

In the case of an initial sinusoidal corrugation with wave-length λ, the preceding "eating up" tendency does not determine the dominant wave-length for some time. However, especially in the case of random initial perturbations, it makes the dominant wave-length in Taylor instability increase with time.

For instance, suppose the interface has random initial perturbations, distributed continuously over a spectrum of wave-lengths. In this case, assuming for simplicity that $\rho' = T = 0$, one can estimate the penetration of the light medium into the dense medium very roughly, as follows: (A rigorous treatment will be given in a later report on the statistics of Taylor instability.)

For each wave-length λ, the existence of mean variations of $A_o = 10^{-3}\lambda$ in elevation seems almost inevitable. Since 10^3 is about e^7, one can therefore expect (by the linear theory of Part II), when $A = e^7 A_o$, a non-linear bubble of wave-length λ to develop. Using Eqs. 12 and 12' with $\rho' = 0$ and $u - u' = T = 0$, this will require a time $t_\lambda = 7\sqrt{\lambda/2\pi a}$. Thereafter, the top of the bubble will rise,

by Sec. 15, with velocity roughly equal to $0.7\sqrt{\lambda a}$. Hence the highest point reached by the light medium should be about

$$Y = \sup_\lambda \left[\lambda + 0.7(t-t_\lambda)\sqrt{a\lambda}\right] \simeq \sup_\lambda \left(0.7t\sqrt{a\lambda} - 2\lambda\right)$$

approximately. For fixed t, the maximum of this quadratic function of $\sqrt{\lambda}$ occurs when $\sqrt{\lambda} = 0.7\ t\sqrt{a}/4$, or the dominant $\lambda_d \simeq 0.03\ a\ t^2$. Substituting back, we get

$$(25) \qquad Y \simeq 0.6\ a\ t^2, \quad \text{with} \quad \lambda_d \simeq .03\ a\ t^2.$$

Thus the predicted bubble penetration Y is about 12% of the asymptotic "spike" penetration.

It is interesting to compare these very rough calculations with experiment. In Ref. 12, Fig. 8, when $a \simeq 1.3 \times 10^5$, the observed $\lambda \simeq 0.8$ cm and $y \simeq 1.0$ cm at $t = 0.011$ sec, as compared with predictions of $\lambda \simeq 0.4$ cm and $Y \simeq 0.8$ cm. At $T = 0.021$ sec the observed $\lambda \simeq 1.5$ cm and $Y \simeq 2$ cm, as compared with predicted $\lambda \simeq 0.8$ cm and $Y \simeq 3.2$ cm.

19. General Density Ratio.

We now pass to Stages (2) and (3) of the case $\alpha \neq 1$ of a general density ratio $\rho' \neq 0$. The experimental observations of Allred (Ref. 1) and Duff (Ref. 7) indicate that the development of Taylor instability in the case $\rho' > \rho/2$ $(0 < \alpha < 1/3)$ differs in two respects from the case $\rho' << \rho$. First, the round-ended rising columns of the lighter liquid are no longer separated by narrow falling spikes or

curtains, but are separated by round-ended falling columns of somewhat similar shape. And second, the rate of fall in Stage (3) is no longer expressed by $g(t - t_o)$, but grows much more slowly, say* like $\alpha\, g(t - t_o)$ or $C(t - t_o)^{1/2}$.

Qualitatively, the preceding changes can both be explained. Thus, it is shown in Appendix A that as $\alpha \downarrow 0$, symmetry under reflection in a horizontal plane tends to be preserved, even for corrugations of large amplitude (cf. Ref. 7, p. 6). Again, Helmholtz instability should tend to flatten out the tip of a spike as it descends (Ref. 4, p. 14), thereby increasing the resistance to its fall. This effect is very pronounced in the case of a sphere moving through a liquid**: it has been observed that an oil globule in water will flatten and "dish out" after a few diameters of travel; successive cross-sections are sketched in Fig. 6. This is due, of course, to the underpressure zone

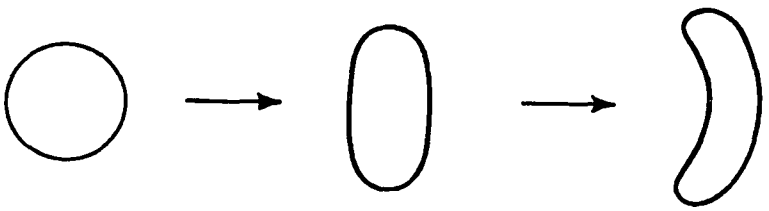

Fig. 6

*Unfortunately, not much data is carefully analyzed in Refs. 1 and 7 so as to give quantitative information on this point. See Ref. 1, Figs. 4.16-4.19, for the roundedness of the columns; Ref. 7 is even more graphic. Although Ref. 1, Fig. 4.13, suggests $v \alpha (t - t_o)$, Russell Duff says $v \alpha (t - t_o)^{1/2}$ in his SF_6 data: "Observations of Taylor instability in gases", paper presented to Am. Phys. Soc., Jan. 1954. It would be very desirable to get more exact data.

**See G. Birkhoff and T. E. Caywood, J. appl. phys. 20 (1949) p. 659, Fig. 15. Unpublished photographs show the effect much more clearly.

at the "equator", and not to the acceleration field, which would leave the sphere rigid (Sec. 6).

It should be noted that most theoretical estimates* predict a "free fall" velocity, for general α, like $\alpha g(t - t_o)$ or $(\rho - \rho') g(t - t_o)/\rho$. But the author thinks that the arguments advanced are only valid for, say, $\alpha > 1/2$, $\rho > 3\rho'$. See Sec. 20 for a further study of this point.

20. Spikes or Curtains.

Consideration of the formulas of Sec. 15 leads one to the conclusion that, in stable steady motion, rising bubbles should have spherical tips -- i.e., circular cross-sections. In particular, two-dimensional bubbles should be unstable. For, letting $\kappa_1 > \kappa_2$ be the principal curvatures of a bubble tip, the pressure gradient normal to the bubble will be greater in the κ_1 - direction. Since the pressure is constant in the bubble, this gives an excess liquid pressure in the κ_1 - direction, which will cause flow towards the κ_2 - direction, tending to equalize κ_1 and κ_2. Experimentally, with ordinary bubbles, the tendency to spherical symmetry seems indeed to occur.

This question covers one phase of three-dimensional Taylor instability. It indicates that, near the top of the interface, a horizontal section will consist of near-circles of the lighter fluid separated by walls of the heavier fluid. Somewhat further down, these

*D. S. Carter, PNJ-LA-6; E. Fermi and J. von Neumann, TM-106; G. M. Carrier, Official Memorandum (1953); formula (2.9). Also, G. Birkhoff, Quar. Appl. Math. 12 (1954), 306-9.

walls will presumably thin out into curtains.

If $\rho' << \rho$, it may be expected that these curtains will "fall" freely for some time, so that the shape of the interface roughly resembles a two-dimensional honeycomb. If ρ' and ρ are comparable (say, if $\alpha < 1/2$), the thicker walls should fall fastest, gradually becoming "spikes" of limited length and circular cross-section. Thus, if $\alpha < 1/2$, one might expect a horizontal section towards the bottom of the interface to be dual to that near the top. Towards the bottom, such a section should consist of near-circles of the (falling) heavier fluid separated by walls of the lighter fluid.

In the case of a random initial perturbation, the interface will have an especially complicated shape.

21. Duration of Stage (3).

There are two factors limiting the duration of Stage (3): the resistance of the lighter fluid to a spike or curtain falling through it, and Helmholtz instability. Both are increasingly effective as ρ'/ρ tends to one.

First, consider the steady fall in Stage (3) of a "narrow upstanding column" (Sec. 3) or curtain. The discharge per unit time is $v\lambda$, where v is the rate of rise of the "round-ended column". By Sec. 15, $v\lambda$ is roughly $\sqrt{a\lambda^3}$. Again, at a depth $L = \frac{1}{2} a t^2$, the velocity of free fall is $v_1 = at$; hence the thickness of the curtain is about

$$\delta = (v\lambda)/v_1 = (\lambda^3/at^2)^{1/2} .$$

Again by Sec. 15, the pressure gradient near the tip of the curtain is about $\rho' v_1^2/\delta$ outside; it is ρ a inside. Equating, we get the limiting relation

$$\rho a \geq \rho' v_1^2/\delta = \rho' v_1^3/(v\lambda) = \rho' a^3 t^3/\sqrt{a\lambda^3}.$$

Simplifying, $(\rho/\rho') \geq (at^2)^{3/2} \sqrt{\lambda^{3/2}} = (2L/\lambda)^{3/2}$, or

$$L/\lambda = 0.5(\rho/\rho')^{2/3}. \tag{26}$$

Thus, with an air-water interface, $L \leq 40\lambda$.

As regards Helmholtz instability, we again refer to Kelvin's perturbation equations, Eqs. 12 and 12', neglecting a and T, and setting $u' - u = v_1$. Then Eqs. 12 and 12' give essentially $A = A_o e^{\beta k v_1 t} = e^{\beta kL}$, where $\beta^2 = \rho\rho'/(\rho+\rho')^2$. Thus, $A = e^7 A_o \simeq 1000 A_o$ when $\beta kL = 7$, or $L = 7\lambda/2\pi\beta \simeq 1.2\lambda/\beta$. With an air-water interface, $\beta \simeq 1/27$. Hence, Helmholtz instability should give non-linear perturbations of wave-length λ when $L \simeq 30\lambda$, except insofar as surface tension is a stabilizing factor. With a liquid-liquid interface, Helmholtz instability should develop very rapidly indeed, after a free fall of the order of λ.

The ideas just expressed have some experimental confirmation. As regards a liquid-liquid interface, see Ref. 7, Fig. 3 which, however, involves an extraneous periodic wake, as explained in Sec. 11. As regards a water-air interface, Gibson* found bubbles in a cylindrical

*A. H. Gibson, Phil. Mag. 26 (1913), 952-65.

tube of diameter d unstable when their length $L > 20\,d$ or so; they had capillary ripples when $L > 8d$. However, further experiments will be required to establish clearly the limitations on Stage (3) due to Helmholtz instability.

Alternatively, one can inspect experimental data concerning so-called "free turbulent mixing" (Ref. 5, Ch.XIV). A wedge-shaped "mixing zone", whose thickness is about 20% of its length, forms in the case $\alpha = 0$ of fluids of equal density. In the general case of densities $\rho = k\,(1 + \alpha)$, $\rho' = k(1 - \alpha)$, Eqs. 12 and 12' suggest that the thickness of the mixing zone should be about $\rho\rho'/5(\rho + \rho')^2 = \sqrt{1 - \alpha^2}/20$ of its length. In the present case, the relative tangential displacement L would roughly correspond to the length of the mixing zone, giving a thickness $\sqrt{1 - \alpha^2}\ L/20$*.

*For other analogous estimates of the "wiping coefficient", see Los Alamos Scientific Laboratory Reports LA-1593 and LA-1608.

IV. NUMERICAL INTEGRATION OF INITIAL VALUE PROBLEM

22. Critical Introduction.

With the advent of high-speed computing machines, various people have proposed analyzing the effects of Taylor instability, by integrating the differential equations of Sec. 4 numerically, for "typical" initial conditions. Thus, the problem of Taylor instability is interpreted as an "initial value problem" for a suitable system of partial differential equations. We consider first the instantaneous problem of calculating $\partial u/\partial t$, $\partial u'/\partial t$ from u, u'.

At each fixed instant t, the determination of the acceleration potentials $A = \partial U/\partial t$ and $A' = \partial U'/\partial t$ reduces to a linear boundary value problem in potential theory, much as in Secs. 4 and 6. One has, for $\vec{x} \in R \cup R'$ and $\vec{y} \in S$,

$$\nabla^2 A = \nabla^2 A' = 0 \qquad \text{in } R,\ R', \tag{27}$$

$$\partial A/\partial n = \partial A'/\partial n \qquad \text{on } S, \tag{27a}$$

$$\rho A - \rho' A' = F(\vec{y}) \qquad \text{on } S, \text{ where} \tag{27b}$$

$$F(\vec{y}) = \frac{1}{2}\rho' \nabla U' \nabla U' - \frac{1}{2}\rho \nabla U \nabla U + (\rho' - \rho)gy + T\mathcal{K}(\vec{y}), \tag{27c}$$

as in Eqs. 10, 10' and 6. It is known (Sec. 6 and Appendix B) that the

boundary value problem (Eqs. 27-27b) has, for reasonably smooth S and $\vec{F}(\vec{y})$, one and only one solution. Three methods of solving it numerically have been proposed, which may be briefly described as follows.

Method 1. Express the acceleration fields $\vec{a} = \nabla A = \partial \vec{u}/\partial t$ and $\vec{a}' \doteq \nabla A'$ as linear combinations

$$(28) \qquad \sum \dot{c}_n(t)\, \vec{a}_n(\vec{x}) \quad \text{and} \quad \sum \dot{c}_n'(t)\, \vec{a}_n'(\vec{x})$$

of basic harmonic acceleration fields, and try to fit the boundary conditions, Eqs. 27a and 27b.

Method 2. Express the combined acceleration field $\{A, A'\}$ defined on $R \cup R'$ as the potential of an appropriate "vortex layer" of density $\sigma(\vec{y})$ on S. The determination of $\sigma(\vec{y})$ then reduces to the solution of a Fredholm integral equation (see Appendix F for details).

Method 3. Constrain the interface S(t) to belong to a finite-parameter family $S(q_1, \ldots, q_n)$ of configurations. For any $\vec{q}(t)$, one can then calculate the Lagrangian

$$(29) \qquad L[\vec{q}(t)] = \frac{1}{2} \sum T_{\kappa\lambda}(\vec{q})\, \dot{q}_\kappa\, \dot{q}_\lambda - V(\vec{q})$$

associated with the instantaneous configuration S(t) and its various degrees of freedom of deformation. Then the $\ddot{q}_\nu$ can be determined by the usual equations of motion (Ref. 16, Sec. 29)

$$(29a) \qquad T_{\mu\nu}\, \ddot{q}_\nu + [\kappa\lambda, \mu]\, \dot{q}_\kappa\, \dot{q}_\lambda = \partial V/\partial q_\mu\,, \quad \text{where}$$

(29b) $$[\kappa\lambda,\mu] = \frac{1}{2}\left\{\partial T_{\lambda\mu}/\partial q_\kappa + \partial T_{\kappa\mu}/\partial q_\lambda - \partial T_{\kappa\lambda}/\partial q_\mu\right\}$$

(See Ref. 11, Ch. VI and Ref. 3, Ch. V for justification.)

We shall discuss Method 1 in Secs. 23-25, Method 2 in Secs. 26-27, and Method 3 in Secs. 28-30. But first, we shall make some critical comments which apply to all three methods; a fourth method, to be treated in Sec. 31, is of a very different character.

For any fixed t, in principle all three methods seem sound as a means for determining $A = \partial U/\partial t$ and A' from U and U'. This soundness is directly related to the existence and uniqueness theorems which are known to hold for the system of Eqs. 27-27c.

However, no corresponding theorems are known for variable t. If S is analytic at $t = 0$, then analogy* suggests that the initial value problem in question has a unique solution for sufficiently small t. However, the facts for large t are unclear; moreover, it is quite certain that, if surface tension is neglected (mathematically, if $T = 0$ in Eq. 27c), then the perturbation equations of Part II do not have a solution for general $t > 0$: they are irregular.**

From a practical point of view, too, we seem limited, by the

---

*L. Lichtenstein, "Grundlagen der Hydrodynamik", Berlin, 1929, p. 422; also "Einige Klassen von Integrodifferentialgleichungen", Berlin, 1931, p. 133.

**G. Birkhoff, Journal of S.I.A.M. 2(1954),57-67. The existence of surface tension will, however, limit the surface area of S, and make the perturbation equations regular.

speed and storage capacity of existing computing machines, to the case of two space variables (plane or axially symmetric case*), hence to a one-dimensional interface. Even the simplified case of a periodic perturbation of plane motion has defied accurate numerical treatment so far, but it should yield to further effort.

23. First Method, Fixed t.

Method 1 was used by Pennington (Ref. 14) to calculate the growth of periodic Taylor instability, and by Penney and Thornhill (Ref. 13) to calculate the base surge from an atomic bomb. The case of fixed t, $\rho' = 0$, is especially straightforward and we shall consider it first.

In the case of periodic Taylor instability (Fig 7a), we can

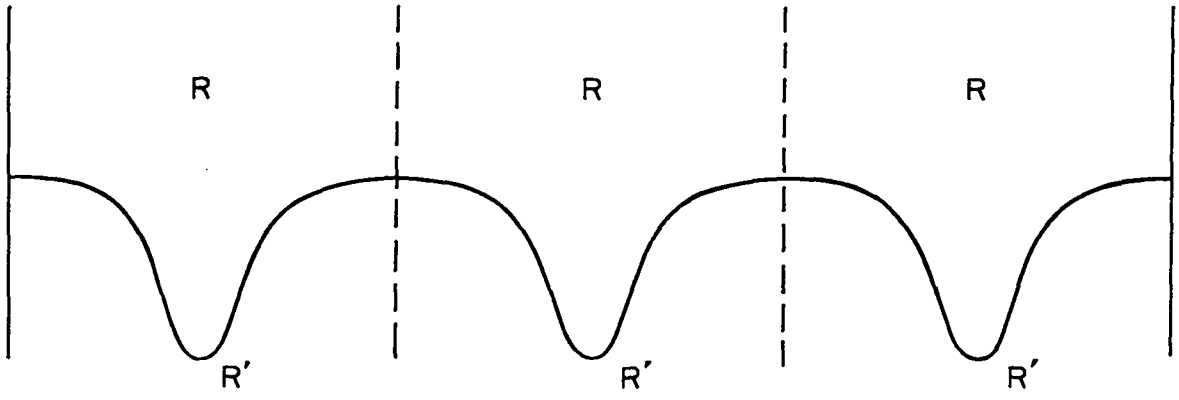

Fig. 7a

normalize to the case of wave-length $\lambda = 2\pi$ by the First Similarity Principle. One can then show that $A = \partial U/\partial t$ and U can be approximated arbitrarily closely by finite linear combinations

*Existence and uniqueness theorems are much easier in this case. See K. Maruhn, Math. Zeits. 45 (1939), 155-84; J. Leray, Jour. de Math. 12 (1933), 1-184; and Acta Math. 63 (1934), 193-248.

$$(30)\qquad U = \mathrm{Re}\left\{\sum_{n=1}^{N} c_n e^{inz}\right\} = \sum_{n=1}^{N} e^{-ny}(a_n \cos nx - b_n \sin nx)$$

$$(30a)\qquad A = \mathrm{Re}\left\{\sum_{n=1}^{N} \dot{c}_n e^{inz}\right\} = \sum_{n=1}^{N} e^{-ny}(\dot{a}_n \cos nx - b_n \sin nx).$$

To prove this, consider the variable $w = e^{iz}$, $z = -i\mathrm{Ln}\, w$, which defines a many-one map of R onto a simply connected domain D in the w-plane. Then finite sums

$$(30b)\qquad U = \sum_{n=1}^{N} c_n w^n, \quad A = \sum_{n=1}^{N} \dot{c}_n w^n$$

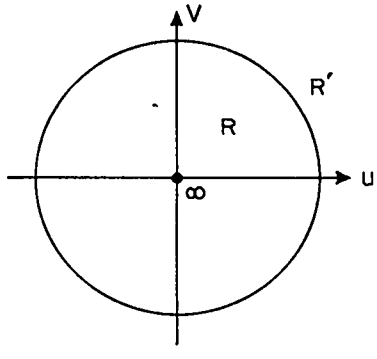

Fig. 7b

are known* to exist, approximating arbitrarily closely to U and $A = \partial U/\partial t$ on D -- or equivalently, by the Maximum Principle, on S.

*J. L. Walsh, "Interpolation and approximation", New York, 1935, Secs. 4.5 and 6.5; Bull. Am. Math. Soc. 35 (1929), 499-544. The existence of polynomial approximations (Eq. 29b) does not of course mean that U can be expanded in a Taylor series.

If U and A are analytic on domains $D^* > D$, then (Walsh, Sec. 5.2) least squares approximation implies uniform approximation. Hence, one can calculate A to any desired uniform approximation by choosing N large enough, and fitting Eq. 27b by a best least squares approximation; the weighting function on S can be arbitrary. This was Pennington's procedure.

A similar argument applies if $\rho' \neq 0$. Assuming the (known) existence and uniqueness theory for Eqs. 27-27c, one can fit the solutions A,A' simultaneously arbitrarily closely. It is less obvious, but probably still true, that least squares approximation implies unfform approximation in this case.

In the case of Penney and Thornhill (Ref. 13), axially symmetric harmonic functions were used and expressed as linear combinations

$$(31) \qquad U = \sum a_n(t)\, r^n\, P_n(\cos\phi),\ A = \sum \dot{a}_n(t)\, r^n\, P_n(\cos\phi)$$

of zonal harmonics. In this case approximation theorems are still known*, but the convergence theory for least squares approximations is less well developed. However, it is noteworthy that Penney and Thornhill used interpolation formulas (Ref. 13, Sec. 4). I know of no theoretical justification for the use of interpolation, even on the sphere, to determine the coefficients of Eq. 31, although equal-spaced inter-

*J. L. Walsh, Bull. Am. Math. Soc. 35 (1929), 499-544, Sec. 7; S. Bergman, Math. Annalen 86 (1922), 238-71 and 98 (1928), 248-63.

polation is known to converge in the analogous case, Eq. 29b, of Fourier expansions* in the unit circle. It would be interesting to recompute the Penney-Thornhill problem, using a least-squares approximation to determine the coefficients in Eq. 30.

24. First Method, Variable t.

When the deformation of the interface S has a large amplitude, the expansions of Eqs.29 and 29a are not very suitable. Thus, if the relative amplitude $A/\lambda = 1$, then $\mathrm{Re}\{e^{inz}\}$ varies by a factor $e^{2\pi N}$ along the interface. If N = 12 terms are taken, the factor is $e^{24\pi} \simeq 10^{32}$. The difficulty of calculating accurately in the presence of such variations in magnitude is obvious.

To avoid this difficulty, one can replace polynomials, in w (Eq. 30b) by polynomials in a related variable such as $w_1 = \sqrt{w-(1+\varepsilon)L} - (1+\sqrt{\varepsilon})\sqrt{-L}$; such polynomials are of less variable magnitude over the flow. This was done in Ref. 14, for the case of an initial sinusoidal perturbation. Step-by-step integration was carried out until the relative bubble penetration $Y/2\pi = 0.25$, the spike fell $L/\pi = 0.75$, giving a total relative amplitude $A/\pi = 1.0$, approximately. It is noteworthy that departures from linearity (e.g., from symmetry under reflection in a horizontal plane) were already marked (Ref. 14, Fig. 5.1) when $Y/2\pi = 0.06$, $L/2\pi = 0.09$, $A/2\pi = 0.15$, which is considerably less than the limit $A/2\pi = 0.4$ estimated in Ref. 12, Sec. 2, Stage (1) . It is also noteworthy that the calculated Y(t) agreed

*D. Jackson, "Theory of Approximation", New York, 1930, p. 123.

closely (Ref. 14, Fig. 5.2) with that calculated by Layzer as in Sec. 17.

However, attempts to make similar calculations for other initial conditions were less successful, giving rise to anomalies when $A/2\pi = 0.2$. Also, substitutions of the form $w_1 = g(w)$, $w_1' = g_1(w)$, would be difficult to correlate in the case of two fluids of comparable density.

Similar difficulties would presumably arise in base-surge calculations, if performed as in Ref. 13 by similar methods. They would be less formidable, because the Nth term in U grows like r^N instead of e^{Ny}. Actually, anomalies appeared by the time the diameter of an initially hemispherical or hemicylindrical column had doubled. Thus, the calculated interface had wavy projections which would not be expected in nature (Ref. 13, Figs. 4-7), and the calculated mass had increased by 6%-12%, and the calculated energy by 20% or more! These anomalies may also have been due to the small number of terms carried (N = 3 or 5).

25. Contact Angle.

In Ref. 13, the angle β between the free boundary and the solid wall caused special trouble. If any finite expansion (Eq. 30) is used, then $\beta = 90^\circ$ necessarily, whereas $\beta = 60^\circ$ in steady flow (Ref. 13, Sec. 4). In this connection, it may be noted that any contact angle β is possible in accelerated flow. Thus, consider the uniformly accelerated flow with U = axt. By the Bernoulli equation (Ref.

11, p. 19),

$$p/\rho + gy + \frac{1}{2}\nabla U \cdot \nabla U + \partial U/\partial t = F(t),$$

which reduces to

$$p/\rho = F(t) - \frac{1}{2}a^2t^2 - gy - ax = F_1(t) - gy - ax.$$

Hence the isobars are the lines $ax + gy = \text{const.}$ making an angle $\arctan(-a/g) = \beta_o$ with the horizontal.

Similar formulas hold in the case of two fluids of different densities ρ, ρ'; the locus

$$(32) \qquad y = (x - at^2/2)\tan\beta_o, \quad \tan\beta_o = (-a/g),$$

is still at constant pressure, hence a possible interface.

This discussion suggests that, as steady motion is approached, the angle of contact β tends to 0° instead of to 60°; this possibility is admitted only parenthetically in Ref. 13, p. 295, footnote. There should be directed experimental evidence in the literature to decide the question.*

26. Second Method, Fixed t.

It is classic (Ref. 11, Secs. 148-149) that a divergence-free vector field, dying off at infinity, is determined by its curl. In the

---

* The case of density currents in hydraulics is not relevant to base surges; with density currents, viscosity and turbulence are the dominating factors. (H. Rouse, "Engineering Hydraulics", p. 763.)

special case of a velocity field defined by two harmonic potential functions, U in R and U' in R', where R and R' are separated by an interface S, the vorticity is all concentrated on the "vortex sheet" S. This is also equivalent to representing the stream function $\{V,V'\}$ on $R \cup R'$ by a "single layer".

We shall consider here only the case of such a spatially periodic, plane velocity field, with wave length π. In this case, if the interface S is represented parametrically by $z = \zeta(a)$, and if ω is the (periodic) vorticity per unit a, so that $\omega = \sigma(\zeta)ds/da$ where $ds = |dz|$, then the complex potential associated with $\omega(a)$ is given by

$$(32^*) \qquad W(z) = \frac{-i}{2\pi} \int_{-\lambda/2}^{\lambda/2} \omega(a)\, \text{Logsin}\,(z - \zeta(a))da.$$

Formula (32*) is derived in Appendix F, where Method 2 is worked out in detail.

Formulas reducing the determination of $\dot{\omega} = \partial\omega/\partial t$ to the solution of a Fredholm integral equation are given in Appendix F and Appendix B. The final equation is

$$(33) \qquad \dot{\omega}(a) = \alpha \int K(\zeta, \zeta')\dot{\omega}(a')da' + H(a),$$

where $$\alpha = (\rho - \rho')/(\rho + \rho'),$$

$$(33a) \qquad K(\zeta, \zeta') = \pi^{-1}\, \text{Im}\left\{\zeta'(a)\cot(\zeta - \zeta')\right\},$$

and H(a) is a function which can be calculated from a given configuration. This is a Fredholm integral equation of the second kind, whose kernel is periodic, The logarithmic singularity of cot ($\xi - \xi'$) on the diagonal $\xi = \xi'$ disappears, because the imaginary part is taken.

In general, it is clear that the numerical solution of Eq. 33 is easiest for small α -- i.e., for the case of nearly equal densities. (In the special case $\rho = \rho'$ of pure Helmholtz instability, $\alpha = 0$, and $\omega(a,t) = \omega(a)$ is time-independent.) Thus Method 2 is especially convenient precisely when Method 1 is least convenient, and most awkward when Method 1 is least difficult, when $\rho' = 0$.

Indeed, Eq. 33 can be solved by direct iteration* for any α, $-1 < \alpha < 1$; the case $\rho' = 0$ is the only exceptional case. However, the convergence of the discretization** does not seem to have been treated rigorously in the literature.

Previous computations (Ref.14) by Method 1 have concerned only the case u = u' of pure Taylor instability, symmetric about the lines x = 0 and $x = \pi/2$. If Method 2 were applied to this case, the Fourier series for $\omega(a,t)$ would have the special form

---

*L. V Ahlfors, Pac. Jour. Math. 2 (1952), 271-80.

**W. Schmeidler, "Integralgleichungen, mit Anwendungen...", Leipzig, 1950, Sec. 22; H. Bückner, "Praktische Behandlung von Integral-gleichungen" Berlin, 1952, Sec. 13. The most relevant papers seem to be those of Bateman and Nyström referred to there. See also F H. Hildebrandt, "Methods of applied mathematics", Ch. IV, and P.D. Crout, J. math. phys. M.I.T. 19 (1940), 34-92.

(34) $$\omega(a,t) = b_1(t) \sin a + b_3(t) \sin 3a + b_5(t) \sin 5a + \ldots,$$

greatly reducing the amount of calculation.

27. Second Method, Variable t.

The case $\alpha = 0$ of pure Helmholtz instability has been calculated by Rosenhead*, using a form of Method 2. Rosenhead discretized the problem by replacing the vortex layer by N equal point-vortices, separated by equal jumps in $\int \omega \, da$. Thus, he reduced the problem to one in the dynamics of particles, which can be solved (Ref. 11, Sec. 154) by integrating the system

$$\dot{x}_1 = - \sum_{k \neq 1} (y_1 - y_k) / \left[(x_i - x_k)^2 + (y_i - y_k)^2 \right]$$

(35)

$$\dot{y}_1 = \sum_{k \neq 1} (x_i - x_k) / \left[(x_i - x_k)^2 + (y_i - y_k)^2 \right]$$

of ordinary differential equations, in suitable units.

Taking N = 8 and N = 12, Rosenhead calculated the development of the vortex system (Eq. 35) up to the point where the vortex layer had twisted through nearly 360°. In Rosenhead's calculation, this

*L. Rosenhead, Proc. Roy. Soc. A134 (1931), 170-92.

twisting or "rolling up" was smooth, and involved no secondary irregularities. However, it may be shown (Appendix F) that Rosenhead's discretization involves assuming a fictitious surface tension. This tends to smooth out the calculations by stabilizing the interface, as already shown in Sec. 9.

Rosenhead's calculations were essentially repeated by D. Carter, with $N = 12, 24$. The interface became irregular after the amplitude had increased to about one-sixth of the wave-length.

28. Third Method.

In Method 3, the configuration R (not the space of velocity-fields, as in Method 1) is supposed constrained by workless constraints to a finite number of degrees of freedom*. Mathematically, this can be represented by the formula

$$z = f(\omega; q_1, \ldots, q_N), \tag{36}$$

where ω is a variable point in a suitable parameter-space, and $q_1, \ldots, q_N$ are generalized coordinates, not to be confused with particle coordinates. In ideal plane flow, it is convenient to let the transformations $f(\omega ; \vec{q})$ be schlicht conformal transformations, representing complex analytic functions.

For any such system, one can define the Lagrangian function

*Method 3, like Method 1, is most convenient in case $\rho' = 0$. For the case $\rho' > 0$, see Appendix G.

(37) $$L = \frac{1}{2} \sum T_{ij}(\vec{q})\, \dot{q}_i\, \dot{q}_j - V(\vec{q}).$$

The potential energy V is easily calculated as

(38) $$V(q) = \frac{1}{2} g \rho \int_S y^2 dx.$$

(To see this, note that the variation $\delta V = g(\rho - \rho') \int y\, \delta y\, dx$, and that $\delta y_1 dx = \delta A$ is the area of the heavier fluid at height $y_1 = y(x_1)$ displacing δA at height $y_2 = y(x_2)$.) The calculation of the kinetic energy tensor $\| T_{ij} \|$ is a little more sophisticated, and involves potential theory.

To calculate $T_{ij}(\vec{q})$, we let U_i, U_i' denote the velocity potentials associated with the motion $\dot{q}_i = 1$, $\dot{q}_j = 0$ if $j \neq 1$. Then

$$U = \sum \dot{q}_i\, U_i, \qquad U' = \sum \dot{q}_i\, U_i',$$

and so as in Ref. 10, Ch. VIII,

(39) $$T_{ij}(\vec{q}) = \rho \int\int_R \nabla U_i \cdot \nabla U_j\, dR = \rho \int_S U_i \frac{\partial U_j}{\partial n} ds = \rho \int_S U_j \frac{\partial U_i}{\partial n} ds.$$

(If $\rho' \neq 0$, $T_{ij}(\vec{q})$ involves also a similar term in ρ', integrated over R'.)

The calculation of $\partial U_i / \partial n = - \partial U'_i / \partial n$ is straightforward. It is the (particle) velocity-component normal to S, away from R.

Again, it is obvious geometrically that this is the same as the normal velocity-component of S. To calculate this, note that if q_i changes by dq_i, all q_j $(j \neq i)$ staying fixed, then the displacement of S is $(\partial z/\partial q_i)dq_i$; hence the normal velocity-component of S is the normal component of $(\partial z/\partial q_i)\dot{q}_i$. This normal component is easily found by trigonometry, since the tangent to S is in the direction of $dz = (dz/d\omega)d\omega_t$, where $d\omega_t$ is tangent to the boundary of the parameter-domain.

Finally, we note that, by the theory of conjugate functions, $\partial U/\partial n = \partial V/\partial s$. Hence $T_{ij} = \int U_i \, dV_j = \int U_j \, dV_i$, and U is the conjugate of the integral V of $\partial U/\partial m$. (This is sometimes referred to as the Dini transform of $\partial U/\partial n$.) From the preceding analysis, $T_{ij}(\vec{q})$ can always be calculated in principle. We shall now consider two special cases, in which the specific calculations are especially elegant mathematically.

29. Polygonal Constraints.

First, we shall suppose that the interface is constrained to be polygonal. Since any curve can be approximated arbitrarily closely by a broken line, it is plausible that, if sufficiently many sides are taken, this will give a good approximation to the unconstrained case.

For simplicity, we shall restrict attention here to the periodic case, and shall further assume that $\rho' = 0$. (For the general case, see Appendix G.) By choice of units (Sec. 5), we can then reduce to the case that $\rho = 1$ and the wave-length $\lambda = 2$, so that a half-

period comprises a strip of width 1, as in Fig. 8.

If $z_i = x_i + iy_i$ $[i = 0, i,\ldots,n]$ denotes the (complex) position coordinate of the ith hinge (vertex), then the potential energy V is simply

$$V = (g/6) \sum_{i=1}^{N} (y_{i-1}^2 + y_{i-1}\, y_i + y_i^2)\, \Delta x_i, \tag{40}$$

where $\Delta x_i = x_i - x_{i-1}$. To compute the kinetic energy T is however much harder.

To compute T, we map R conformally onto the upper half of an auxiliary ζ-plane by a Schwarz-Christoffel transformation, (Ref. 10, p. 370), so that z_o, z_N, ∞ go respectively into $\zeta = 0, 1, \infty$. Correspondingly, we take for our "generalized coordinates" q_i the transforms $\alpha_1,\ldots,\alpha_{N-1}$ of $z_1,\ldots,z_{N-1}$ (clearly, $0 < \alpha_1 < \ldots < \alpha_{N-1} < 1$, as in Fig. 9), and the μ_i giving the "turning angles" $\pi\mu_i$ at the vertices z_i. This gives

$$z = ih + \int_0^{\zeta} d\zeta/R(\zeta), \quad \text{where} \tag{41}$$

$$R(\zeta) = \sqrt{\zeta(1-\zeta)}\ (1-\zeta)^{-\phi/\pi} \prod_{i=1}^{N-1} (a_i - \zeta)^{\mu_i},$$

and $\phi_j = \pi \sum_{i=1}^{j-1} \mu_i$. Here h is real and A real and positive;

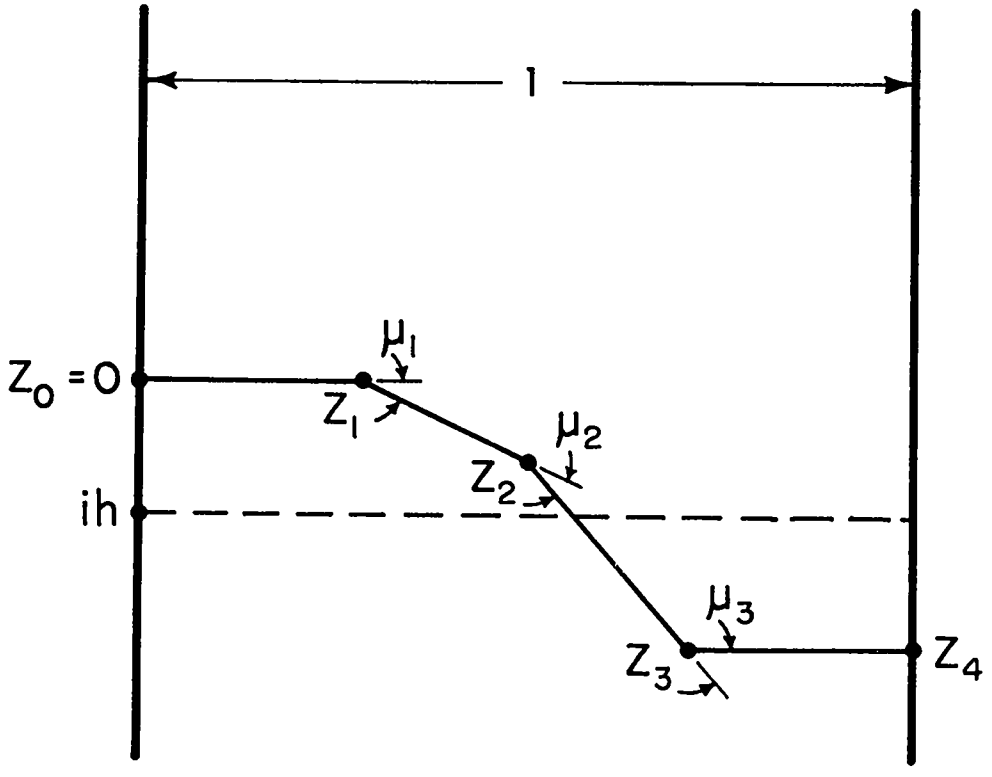

Fig. 8

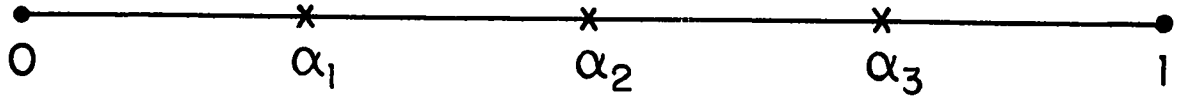

Fig. 9

A is chosen by demanding that $x_n = 1$, and h by volume conservation (zero velocity at infinity).

The special case N = 2, $\mu_1 = 1/2$, $\mu_2 = -1/2$ was treated approximately by Fermi (Ref. 8). In this case, z is given in closed form as an elliptic integral, but the possibility of making exact calculations, using this fact, has not been explored. The case N = 1 has been treated approximately by Judd*. The formulas that follow apply to the general case.

The lengths ℓ_i of the weightless rods composing the interface are given by the real integrals

$$(42) \qquad \ell_i = AI_i, \text{ where } I_i = \int_{\alpha_{i-1}}^{\alpha_i} d\xi / |R(\xi)| \qquad [i = 1, \ldots, n].$$

From Eq. 42 and trigonometry, A is given by

$$(43) \qquad A = \left(\sum_{i=1}^{N} I_i \cos \phi_i \right)^{-1} .$$

Since the sensed area between the line y = 0 and the interface is zero, and $x_n - x_o = 1$, h equals the sensed area between $y = y_n$ and the interface. Hence (cf. Fig. 10) h is given by

$$(43') \qquad 4h = \sum_{i=1}^{N} (x_{i-1} + x_i) \ell_i \sin \phi_i .$$

*Letter dated July 10, 1952.

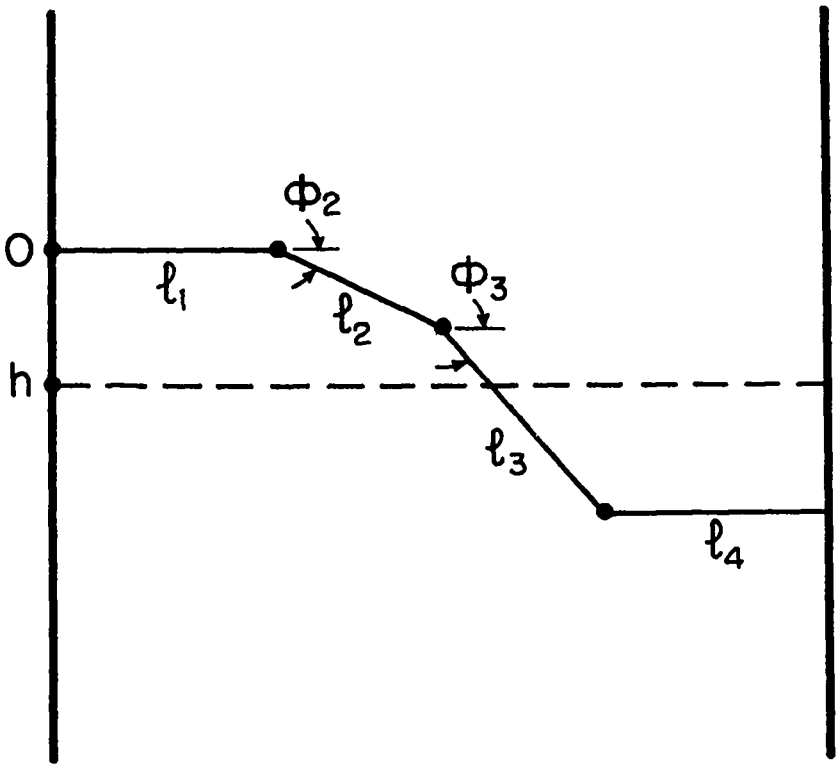

Fig. 10

The following equations are evident:

(44a) $$d\phi_o = 0, \quad d\phi_i = \pi(d\mu_i + \ldots + d\mu_{i-1}),$$

(44b) $$d\ell_i = A\,dI_i + I_i\,dA, \quad dA = -A^2(-I_i \sin\phi_i\, d\phi_i + \cos\phi_i\, dI_i)$$

(44c) $$dx_i = dx_{i-1} + (\cos\phi_i\, d\ell_i - \ell_i \sin\phi_i\, d\phi_i)$$

(44d) $$dy_o = dh \text{ and } dy_i = dy_{i-1} + (\sin\phi_i\, d\ell_i + \ell_i \cos\phi_i\, d\phi_i).$$

On the ith segment at a distance s from its base, the inward normal velocity is clearly a linear function $\partial U/\partial n\ (a_{i\lambda} + b_{i\lambda}\, s)\dot{q}_\lambda$ of the distance $s = |z - z_{i-1}|$, where the $a_{i\lambda}$ and $b_{i\lambda}$ are independent of s. It also equals $-\sin\phi_i[\dot{x}_i s + \dot{x}_{i-1}(1 - s)] + \cos\phi_i[\dot{y}_i s + y_{i-1}(1 - s)]$. Therefore $a_{i\lambda}$ and $b_{i\lambda}$ are given as functions of q by

(45a) $$a_{i\lambda} = -\sin\phi_i \frac{\partial x_{i-1}}{\partial q_\lambda} + \cos\phi_i \frac{\partial y_{i-1}}{q_\lambda}$$

(45b) $$b_{i\lambda} = -\sin\phi_i \frac{\partial(\Delta x_i)}{\partial q_\lambda} + \cos\phi_i \frac{\partial(\Delta y_i)}{\partial q_\lambda},$$

where $\Delta x_i = x_i - x_{i-1}$ and $\Delta y_i = y_i - y_{i-1}$.

Expressions for the partial derivatives involved in Eq. 45a and 45b are given in Appendix G. Using the known formula for U in

terms of $\partial U/\partial \nu = (\partial U/\partial n) \cdot |dz/d\zeta|$ in the upper half-plane, one can deduce also

$$(46) \qquad T_{\kappa\lambda} = -\frac{1}{\pi}\int_0^1\int_0^1 \frac{\mathrm{Ln}\,|\xi - \xi'|}{|R(\xi)|\cdot|R(\xi')|}\,\frac{\partial U_\kappa}{\partial n}(\xi)\,\frac{\partial U_\lambda}{\partial n}(\xi')\,d\xi\,d\xi'$$

$$= -\pi^{-1}\iint \mathrm{Ln}\,|\xi - \xi'|\,\frac{\partial U_\kappa}{\partial n}(\xi)\,\frac{\partial U_\lambda}{\partial n}(\xi')\,ds\,ds',$$

by Eq. 41. By expanding the preceding formulas, the Lagrangian $L(\vec{q})$ can be computed; the details are in Appendix G.

30. Harmonic Constraints.

We next let the parameter domain be the unit circle $\omega = re^{i\sigma}$ $(0 < \sigma < 1)$, and the configuration $R = R(\vec{q})$ be given by

$$(47) \qquad iz = \mathrm{Ln}\,\omega + q_0(t) + q_1(t)\omega + q_2(t)\omega^2 + \ldots + q_N(t)\omega^N.$$

For complex q_i, summed from $i = 0$ to $i = \infty$, this would represent the most general periodic displacement of the region $y > 0$, with wavelength $\lambda = 2$. For simplicity, we consider only the case of real $\vec{q}$, with $a = \rho = 1$ and $\rho' = 0$. In this case, $iz(\omega^*) = -iz^*(\omega)$, hence $x(\omega^*) = -x(\omega)$ and $y(\omega^*) = y(\omega)$. Thus the case of real $\vec{q}$ corresponds to symmetry in the vertical line $x = 0$ (and its periodic translates $x = \pm 2n\pi$).

The case $q_2 = q_4 = \ldots = 0$ is also of interest. In this case $\sin k(2\pi - \sigma) = -\sin k\sigma$ for k odd, etc., and so

$$iz(re^{i(2\pi-\sigma)}) = \text{Ln } r + 2\pi i + q_o - i\sigma + \sum q_k r^k(\cos k\sigma - i \sin k\sigma)$$

Hence, $iz(re^{i(2\pi-\sigma)}) = 2\pi i + [iz(\omega^*)] = i(2\pi - z(\omega^*))$. That is, the case $q_{2K} = 0$ of odd coefficients is the case of symmetry in the vertical lines $x = 0, \pm\pi, \pm 2\pi, \ldots$. Thus, it contains the case treated by Taylor and Lewis (Refs. 15, 12).

The condition $\oint y dx = 0$ of zero mean vertical displacement (here $\oint$ refers to integration ever a complete period) is easily expressed in terms of $\vec{q}$. Since

$$(47') \qquad x = \sigma + \sum_{k=1}^{N} q_k \sin k\sigma, \quad y = -q_o - \sum_{k=1}^{N} q_k \cos k\sigma \quad \text{on S},$$

the condition is

$$(48a) \qquad 2q_o = -\sum_{k=1}^{N} k\, q_k^2.$$

The potential energy V per period is also easily expressed in terms of $\vec{q} = (q_o, \ldots, q_N)$. By Eq. 38, since $g = 1$, $\rho = 1$ and $\rho' = 0$,

$$V = \frac{1}{2}\oint y^2 dx = \frac{1}{2}\oint \sum_{h,k} q_h q_k \cos h\sigma \cos k\sigma \sum_{l} l q_l \cos l\sigma \, d\sigma .$$

But the integral is $\pi/2$ if $h \pm k = \ell$, and zero otherwise. Hence

$$V = \frac{\pi}{4} \sum_{h \pm k = \ell} \ell q_h q_k q_\ell \quad . \tag{48b}$$

To calculate the kinetic energy T, we first relate $\partial U/\partial n$ in the z-plane to $\partial U/\partial \nu = \partial U/\partial r$ in the ω-plane by the formula $\partial U/\partial \nu = |dz/d\omega| \, \partial U/\partial n$, which is evident from the conformality of $z(\omega)$. But now, the tangent direction to the interface S is, at any point, given by $\partial z/\partial \sigma$, or

$$\partial x/\partial \sigma = 1 + \sum_{k=1}^{N} k q_k \cos k\sigma, \quad \partial y/\partial \sigma = \sum_{k=1}^{n} k \, q_k \sin k\sigma .$$

The velocity on the boundary is $\dot{z} = \sum (\partial z/\partial q_k)\dot{q}_k = -i \sum \dot{q}_k \, e^{ik\sigma}$. From these two formulas, $\partial U/\partial n$ is easily calculated as the component of $\dot{z}$ normal to $\partial z/\partial \sigma$, whence so is $\partial U/\partial \nu = |dz/d\omega| \, \partial U/\partial n$, where

$$|dz/d\omega| = \left| \omega^{-1} + \sum k \, q_k \, \omega^{k-1} \right| .$$

But, knowing $\partial U/\partial \nu = \sum c_k \cos k\sigma$, numerical quadrature gives

$$2T = \oint U \frac{\partial U}{\partial \nu} d\sigma = \iint |dW/d\omega|^2 \, r \, dr \, d\sigma = \pi \sum k^{-1} c_k^2 ,$$

as in Ref. 5, Ch. VI, Eq. 14d.

$$2T = \iint D(\sigma, \sigma') \frac{\partial U}{\partial \nu}(\sigma) \frac{\partial U}{\partial \nu}(\sigma') \, d\sigma \, d\sigma' , \tag{49a}$$

where

$$(49b)\quad D(\sigma, \sigma') = \frac{2}{\pi} \sum_{j=1}^{\infty} \frac{\sin j\sigma \sin j\sigma'}{j} = \frac{1}{\pi} \operatorname{Ln} \left| \frac{\tan \sigma/2 + \tan \sigma'/2}{\tan \sigma/2 - \tan \sigma'/2} \right| .$$

Equations 49a and 49b are analogous to Eq. 46; even more analogous would be

$$(49c)\quad 2T = \iint D(\sigma, \sigma') \left| dz/d\omega \right|^2 \frac{\partial U}{\partial n}(\sigma) \frac{\partial U}{\partial n}(\sigma')\, d\sigma\, d\sigma'$$

$$= \iint D(\sigma, \sigma') \frac{\partial U}{\partial n}(\sigma) \frac{\partial U}{\partial n}(\sigma')\, ds\, ds'.$$

Although no calculations using the preceding equations have yet been carried through, I would guess that the numerical work would proceed more smoothly than if the polygonal constraints of Sec. 29 were used.

31. Ulam-Pasta Method.

The development of Taylor instability and mixing can also be studied by considering the motion under gravity and mutual repulsion of mass-particles of different weights. Using the ideas of the kinetic theory of gases, a system of such particles of equal mass may be regarded as constituting a homogeneous gas of appropriate density and pressure. An interface separating particles of different masses can be given an arbitrary initial configuration, and its development followed.

This scheme has been effectively used by S. Ulam and J. Pasta (unpublished Los Alamos Scientific Laboratory report); it is convenient

to use $1/r$ or mm'/r repulsion law, with a "cutoff" making forces vanish if $r > R$, a fixed radius. It has the advantage of being applicable to compressible fluids.

Calculations were made with initially 16 rows of 16 particles. The top 7 rows consisted of heavy particles; the 8th row of 7 light particles followed by 9 heavy particles; the 9th row of 8 light followed by 8 heavy particles; the 10th row of 9 light followed by 7 heavy particles; the 11th-16th rows of light particles. Fig. 11 shows the configuration at two instants, after considerable time has elapsed.

The disadvantages of the method are, that it does not apply to the case of incompressible fluids, and that the quantitative interpretation of the results is difficult.

[Added in proof. See LA-1557 (June 1953) for related remarks. For still another approach, see R. L. Ingraham, Proc. Phys. Soc. London, B67 (1954), 748-52.]

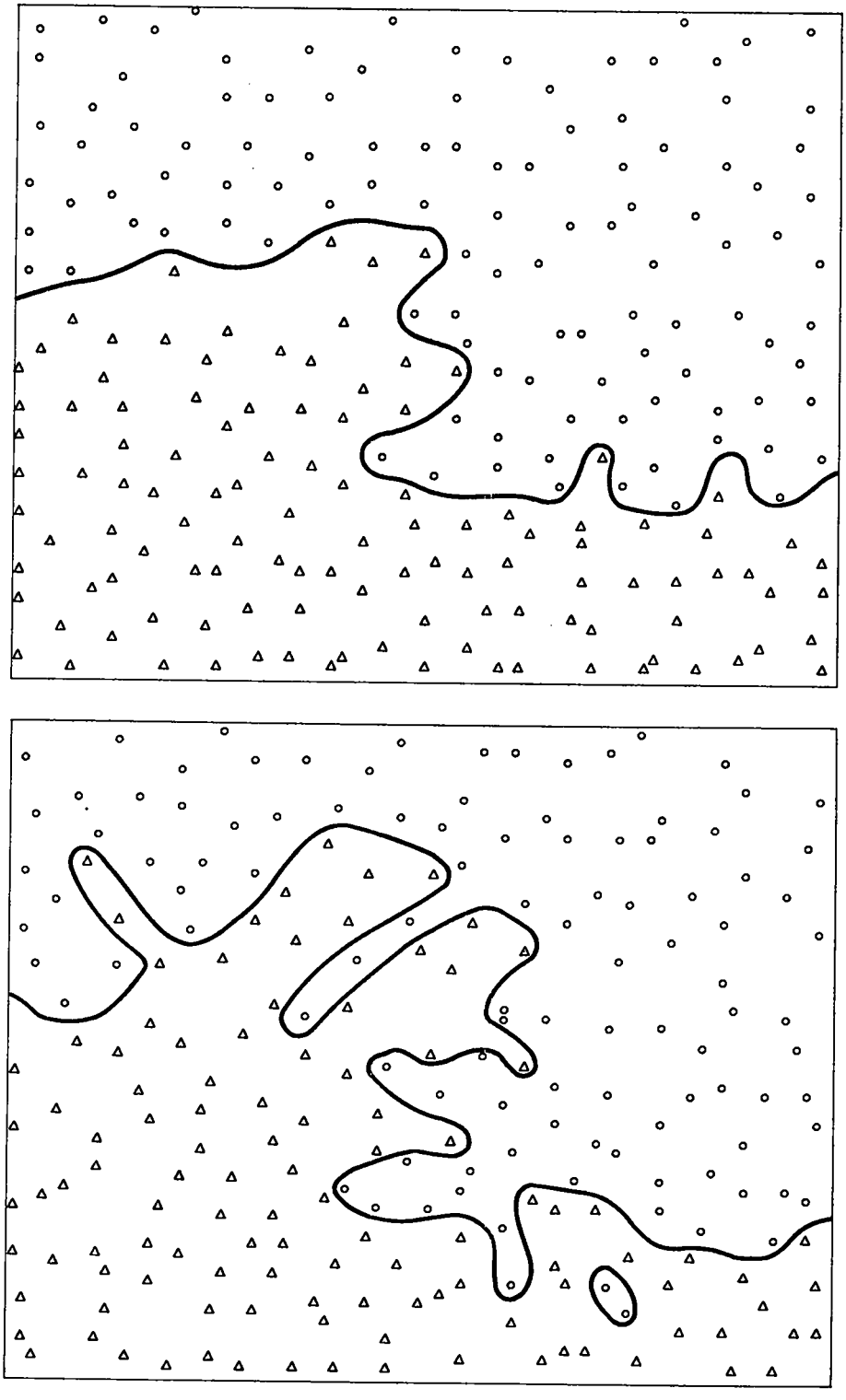

Fig. 11

REFERENCES

(1) J. C. Allred and G. H. Blount, "Experimental studies of Taylor instability", Report LA-1600, 1953.

(2) R. Bellman and R. H. Pennington, "Effects of surface tension and viscosity on Taylor instability", Quar. Appl. Math. 12 (1954), 151-62.

(3) G. Birkhoff, "Hydrodynamics, a study in logic, fact and similitude", Princeton University Press, 1950.

(4) G. Birkhoff and R. H. Ingraham, "Taylor instability", Report under Subcontract SC-7, 1952.

(5) G. Birkhoff and E. H. Zarantonello, "Jets, Wakes and Cavities", to be published.

(6) J. W. Calkin, "Mixing of frictionless, incompressible substances, I", Report LA-1472, 1952.

(7) R. E. Duff and H. T. Knight, "Progress report on Taylor instability studies", Report GMX-R-110, 1953 (not available).

(8) E. Fermi, "Taylor instability of an incompressible liquid", Los Alamos Scientific Laboratory, September, 1951, reproduced in Appendix G of the supplement to this report.

(9) H. Helmholtz, "Uber discontinuierliche Flüssigkeitsbewegungen", Monatsber. Berlin. Akad. (1868) 215-228. Reprinted in Phil. Mag. (1868) and in Wiss. Abh. 1 (1882).

(10) O. D. Kellogg, "Foundations of potential theory", Berlin, Springer, 1929, and Cambridge, Mass., Murray Printing Co., 1943.

(11) H. Lamb, "Hydrodynamics", 6th ed., Cambridge University Press, 1932.

(12) D. J. Lewis, "The instability of liquid surfaces when accelerated in a direction perpendicular to their planes, II", Proc. Roy. Soc. Lond. A202 (1950) 81-96.

(13) J. C. Martin, W. J. Moyce, W. G. Penney, A. T. Price, and C. K. Thornhill, "Some gravity wave problems in the motion of perfect liquids", Phil. Trans. A244 (1952), 231-334.

(14) R. Pennington, "Machine calculation of the growth of Taylor instability in an incompressible fluid", Report PNJ-LA-11, undated.

(15) G. I. Taylor, "The instability of liquid surfaces when accelerated in a direction perpendicular to their plane, I", Proc. Roy. Soc. Lond. A201 (1950), 192-196.

(16) E. T. Whittaker, "Analytical dynamics", Cambridge University Press, 4th ed., 1937.

LIST OF APPENDICES

Appendix A. Remarks on similarity.

Appendix B. Impulsive acceleration.

Appendix C. Stability of heterogeneous fluids.

Appendix D. Steady state bubble rise.

Appendix E. Remarks on Layzer's model.

Appendix F. Calculation of interface motion, via associated vortex layer.

Appendix G. Motion of a polygonal interface (Fermi model).

These Appendices will be issued later as LA-1927, a supplement to the present report.